HYDROLOGIC IMPACTS OF DUST ON SNOW

IN THE UPPER COLORADO RIVER BASIN

by

Ann Bryant Burgess

A dissertation submitted to the faculty of
The University of Utah
in partial fulfillment of the requirements for the degree of

Doctor of Philosophy

Department of Geography

The University of Utah

May 2014

The University of Utah Graduate School

STATEMENT OF DISSERTATION APPROVAL

The dissertation of **Ann Bryant Burgess**

has been approved by the following supervisory committee members:

Richard R. Forster	, Chair	**Nov 8, 2013** Date Approved
Thomas H. Painter	, Member	**Nov 8, 2013** Date Approved
Philip E. Dennison	, Member	**Nov 8, 2013** Date Approved
Thomas J. Cova	, Member	**Nov 8, 2013** Date Approved
Jeffery S. Deems	, Member	**Nov 8, 2013** Date Approved

and by **Andrea R. Brunelle**, Chair of the Department of **Geography**

and by David B. Kieda, Dean of The Graduate School.

ABSTRACT

Water availability is one of the most pressing scientific and societal issues facing the western United States. By 2060, population within the Colorado River Basin is expected to grow 19-48% relative to the 2010 population, significantly increasing the demand for water. Simultaneously, streamflow in the Colorado River is projected to decrease between 5-20%, putting further strain on an already over-allocated system. The high-elevation snowpack of the Upper Colorado River Basin (UCRB) contributes the majority of runoff to the Colorado River through winter snow accumulation and springtime snowmelt. Recent studies have shown however, that dust from the Colorado Plateau shortens snowcover duration in the southeastern portion of the UCRB by 25-51 days. By accelerating snowmelt and extending the snow-free season, this impact appears to have shifted peak normalized runoff at Lee's Ferry, AZ 3-6 weeks earlier and reduced the total annual runoff of the Colorado River by 5-6% relative to the cleaner-snow conditions that existed prior to the western expansion of the United States in the mid-1800s.

The agency charged with monitoring and forecasting streamflow in the UCRB is the Colorado Basin River Forecast Center (CBRFC). The CBRFC predicts snowmelt runoff using the temperature-index based SNOW-17 model that assumes an empirical relationship between temperature and snowmelt. The melt factor used in SNOW-17 is effectively a calibrated index of the relative proportions of snow surface energy balance components over the model's calibration period. If energy balance components deviate

from the calibration-period mean, however, the fraction of radiation absorbed by the snowpack can also shift, influencing snowmelt timing and runoff and rendering the melt index less representative. Based on observations and in situ measurements, we know that dust deposition varies annually and spatially throughout the UCRB. The work described herein is directed at improving our understanding of the spatial and temporal variability of dust radiative forcing in snow and ultimately how that variability impacts streamflow forecasting in the UCRB.

I would like to dedicate this dissertation to my family,

who fostered curiosity for the world and joy in its exploration.

...and to Evan, I don't know how anyone does this without sharing an office with their greatest love.

TABLE OF CONTENTS

LIST OF FIGURES

ACKNOWLEDGEMENTS

I'd like to thank my advisor Tom Painter. On our first field excursion he drew a hydrograph in the loose soils of the Milford Flat using a borrowed screw driver, on the way back to Salt Lake City he grilled us about remote sensing terminology. That set the tone of my graduate experience—he's truly a preacher and a teacher of snow hydrology. I thank him for freedom, funding, and so many opportunities to grow as an academic and professional. I'd also like to thank Rick Forester for his support and thoughtfulness throughout my tenure at Utah – it is truly appreciated. I thank Jeff Deems and Chris Landry for their insight and support over the years and McKenzie, a great field partner and friend. To Cam and the rest of the JPL Snow crew, I wouldn't want to chat for hours and hours with any other computer science/software developer dream team! A big thanks to Stacie Bender for endless SNOW-17 enumeration, data sharing, and enthusiasm about our collaboration – this body of work truly would have been impossible without you. Thank you to everyone else at the CBRFC for their time and effort helping me better understand how streamflow forecasting works in the intermountain west – you are charged with a grand task! Finally, I'd like to thank Rob Brown, Kathleen Schroeder, Mike Mayfield, and Gabrielle Katz – you created an academic environment that I so wanted to be a part of. So much so, ironically, its what made me leave and pursue a PhD. For that, I'm forever grateful.

CHAPTER 1

INTRODUCTION

Among the major river basins of the western US, the Colorado River Basin (CRB) has the most complete allocation of its water resources and is one of the most regulated. Annually, this over-allocated system supplies water to 7 mostly-arid states and Mexico for agricultural, municipal, and domestic consumption [*Barnett and Pierce*, 2009]. By 2060, population within the Colorado River Basin is expected to grow between 19% and 48% relative to the 2010 population [*U.S. Dept. of Int.*, 2013], further increasing the demand for water. Simultaneously, stream flow in the Colorado River is projected to decrease between 5 and 20% [*Vano et al.*, 2012; *Deems et al.*, 2013a], putting further strain on the already-tenuous water supply.

In this over-allocated basin, our ability to monitor and forecast runoff under a wide range of hydroclimatic conditions is imperative. While observational systems (e.g. SNOTEL) provide near-real time in situ data of snowpack conditions, they are not representative of larger-scale conditions. In contrast, operational forecasting provides spatially-comprehensive data, but is dependent upon index methods and therefore sensitive to conditions that fall outside the those represented during their calibration period, such as those caused by anthropogenic climate change [*Mote et al.*, 2005; *Barnett et al.*, 2008; *Vano et al.*, 2012] and deposition of mineral dust on snow [*Painter et al.*,

2007; *Painter et al.*, 2010]. Therefore, progress in representing such conditions would help researchers and the operational forecasting community better understand observed snowmelt patterns and snowmelt-driven streamflow prediction errors.

1.1 Snow Accumulation and Variability

The snowpack of the Upper Colorado River Basin (UCRB) stores 70% of the surface-water runoff for the Colorado River [*Christensen et al.*, 2004]. However, the amount of snow accumulation in the UCRB varies considerably. For any given year, peak snow water equivalent (SWE) depths at snow course sites vary about the long-term mean by 25-60% [*Cayan*, 1996], making Colorado River flows highly variable interannually. The interannual variability is less of a problem for areas further downstream as the major reservoirs of the Colorado River, located near or within the Lower CRB, can store nearly four times its average annual runoff ensuring water availability for the major population centers of the arid southwest [*Vano et al.*, 2012]. But in the UCRB, storage capacity for surface water runoff is relatively limited, leaving water managers and users reliant on the variable high-elevation snowpack for water in the late spring and summer [*Deems et al.*, 2013a]. As such, accurate forecasting of runoff timing and total runoff volume are particularly critical in the UCRB as this region has little storage available to buffer unexpected variations in flow.

Snow accumulation and melt vary on a broad range of spatial scales, on the order of meters to beyond the size of the UCRB. Larger scale spatial variations are dependent on synoptic weather patterns and broad regional topography. On smaller basin scales, local elevation, slope, aspect, and orientation to the larger-scale synoptic patterns control the

uplift of advected moisture and consequently affect orographic precipitation. Wind can also redistribute snowfall on these scales resulting in variations in SWE down to the microscale. This spatial variability leads to distinct challenges in measuring SWE, as point observations (e.g., SNOTEL) may not be representative of the local or basin-scale snowpack, leading to an inescapable level of uncertainty in the use of such observations to estimate SWE [*Fassnacht et al.*, 2003]. Optical remote sensing [*Molotch and Margulis*, 2008; *Rice et al.*, 2011] and LiDAR-based [*Deems et al.*, 2013b] estimates of SWE provide potential for more comprehensive measurements, but are still subject to the temporal, spatial, and vertical variability of snow density measurements that are challenging over large scales. These measurements, however flawed, are critical inputs for hydrologic models that require SWE estimations to drive surface runoff predictions. Because most hydrologic models use empirical relationships between point or grid estimations of SWE and runoff volume (over a given calibration period), they perform best when snowpack conditions are closest to the calibration-period mean [*Bales et al.*, 2006].

1.2 Snow Ablation

As the snowpack grows over the winter, assuming the snow is below freezing, it accumulates what is referred to as cold content which is, by definition, a deficit in total heat content or enthalpy within the snowpack. Since snow has a rather high heat capacity, the snowpack accumulates a large amount of thermal inertia that keeps the snowpack resistant to melting. As spring begins, air temperatures and incoming solar radiation increase, both of which apply heat content to the snowpack and can melt the

surface snow. But before runoff can ensue, enough heat content must be added to the pack to bring all of the snow to the melting point—a process called ripening. This process progresses as surface meltwater percolates through the snowpack and refreezes in colder snow releasing latent heat that adds heat content to colder snow deeper in the pack. Once all of the snow has risen to the melting point, water is able to percolate to the ground, runoff, and contribute to streamflow.

The energy fluxes that contribute to snowmelt can be described by the snow energy balance equation as:

$$\Delta Q+m= (1-a)S+L^{*}+Q_s+Q_v+Q_g \qquad (1.1)$$

where $\Delta Q+m$ is change in snowpack energy plus melt, $1-a$ is 1-albedo and describes absorption of solar radiation S at the snow surface, L^{*} is net longwave radiation, Q_s is sensible heating flux, Q_v is latent heating flux, Q_g is ground heating flux. A negative energy balance cools the snowpack, increasing its cold content or the amount of energy needed to raise the temperature of the snowpack to 0^{o} C. A positive energy balance warms the snowpack and decreases its cold content [*Marks et al.*, 1998].

In midlatitude, continental snowpacks such as the UCRB, net solar radiation is the dominant energy flux driving snowmelt [*Bales et al.*, 2006], where incoming solar radiation is modified by snow surface albedo. Snow surface albedo is a function of snow grainsize and impurity content [*Conway et al.*, 1996]. As the snowpack ripens during springtime ablation, snow grainsize increases causing a coincident decrease in snow surface albedo [*Wiscombe and Warren*, 1980].

1.3 Snowmelt Modeling

All snowmelt models are first and foremost subject to the uncertainties in SWE estimation that drive potential melt volume. Snowmelt models attempt to determine the melt as a function of energy fluxes in and out of the snowpack. Physically based snowpack energy-balance models treat each flux explicitly, while temperature-index based snowmelt models assume an empirical relationship between air temperature and snowmelt [*Anderson*, 1976]. While an idealized spatially-distributed energy balance model would, in theory, produce the most-accurate measure of melt flux [*Marks and Winstral*, 2001], the inputs for such a model are not available at the scale necessary for sufficiently accurate operational melt prediction [*Franz et al.*, 2008]. Therefore, the minimal data requirements, and often-acceptable results, make temperature index models the central component of operational hydrologic forecasting systems where snowmelt dominates regional streamflow.

However, error is introduced into temperature-index models when actual energy-balance conditions deviate from the calibration-period mean. Recent research has shown, that mineral dust transported during episodic events from adjacent arid and semi-arid regions to the UCRB snowpack reduces snow surface albedo, increasing the net solar radiation input into the snowpack, accelerating snowmelt and snowpack depletion [*Painter et al.*, 2007; *Skiles et al.*, 2012]. Further, based on energy balance measurements in southwestern, CO [*Painter et al.*, 2012] and in situ observations [*CSAS*, 2013], we know that dust deposition on snow has considerable spatial and interannual variability throughout the UCRB.

1.4 Dust Deposition on Snow

Dust deposition on mountain snow and ice around the globe has occurred throughout history as demonstrated by annual dust layers in high elevation ice cores [*Thompson et al.*, 2000; *McConnell et al.*, 2007; *Kaspari et al.*, 2009]. These same cores have shown that dust deposition increased in these regions starting in the late 1800s [*Thompson et al.*, 2000; *Kaspari et al.*, 2009] and early 1900s [*McConnell et al.*, 2007], coincident with large scale land-use changes. Similarly, *Neff et al.* [2008] showed that dust deposition in the San Juan Mountains, southwestern CO, US is presently 500% greater than prior to the extensive population and settlement of the western US in the late 1800s, where dust deposition peaked in the period between 1900-1930, coinciding with the maximum number of grazing animals in that region, retreating present day levels after the Taylor Grazing Act of 1934. More recently, *Brahney et al.* [2013] demonstrated an increasing trend in dust deposition in the intermountain west, US between 1992 and 2010, coincident with increased land use and a prolonged period of drought in the region [*Draut et al.*, 2012].

Dust deposition on snow in the San Juan Mountains, CO has been shown to accelerate snowmelt and snowpack depletion by 25-50 days [*Painter et al.*, 2007; *Skiles et al.*, 2012]. Dust accelerates snowmelt because of the optical properties of both dust and snow. Snow without absorbing impurities, such as mineral dust, has the highest albedo of any naturally occurring Earth surface. The spectral albedo of snow over the visible (VIS) through shortwave infrared (SWIR) is attributed to the properties of the "real" and "imaginary" part of the complex refractive index, $N = n+ik$. The real part, $n = c_0/c$, is the ratio of the speed of light in vacuum, c_0, to that in a medium, c, and varies

little for ice over the VIS through SWIR. The imaginary part, k, is defined by $dI/I = -(4\pi k/l)dx$, and describes how radiation of intensity I, at wavelength l, is attenuated as it passes along distance x through a pure medium [*Dozier and Painter*, 2004]. The imaginary part of the complex refractive index for ice is very small in the VIS wavelengths, meaning clean snow scatters, rather than absorbs nearly all-incoming solar radiation. In the near infrared (NIR), however, k_l is roughly five orders of magnitude larger [*Dozier et al.*, 1988], making albedo in the NIR primarily sensitive to grain size [*Wiscombe and Warren*, 1980]. Therefore, the visible albedo of snow decreases if impurities, with stronger absorption characteristics in the VIS, are introduced into the snowpack [*Warren*, 1982] while albedo in the NIR decreases with increasing snow grainsize.

We use the term 'radiative forcing' to describe the combined perturbations that dust has on snowpack energy balance. Radiative forcing is defined by a direct effect and two feedbacks [*Hansen and Nazarenko*, 2004; *Painter et al.*, 2007]. The direct effect is the instantaneous surface-enhanced absorption attributed to absorption of solar radiation by dust in the VIS wavelengths. The first feedback is the increased absorption in the NIR wavelengths by larger-grained snow due to an increased rate of snow metamorphism attributed to the direct effect. The second feedback is the increased absorption by earlier-exposed substrate due to the direct effect and first feedback. Radiative forcing by dust in snow in the UCRB is further driven by two major factors (i) large dust particles (greater than 5.0 μm) accumulate near the snow surface as ablation advances [*Conway et al.*, 1996], and (ii) dust arrives and concentrates during late winter and spring when solar irradiance is increasing [*Painter et al.*, 2007; *Painter et al.*, 2012].

1.5 Hydrologic Impacts of Dust on Snow

While considerable research has been dedicated to understanding the potential impacts of anthropogenic climate change on the Colorado River system [*Christensen et al.*, 2004; *Christensen and Lettenmaier*, 2007; *Barnett et al.*, 2008; *Pierce et al.*, 2008; *Barnett and Pierce*, 2009], these studies have not included the potentially compounding impacts of dust deposition on snow. *Painter et al.* [2010] showed dust on snow (based on 2005 – 2008 dust loading in the San Juan Mountains, CO) has brought peak runoff of the Colorado River at Lee's Ferry 3 weeks earlier than prewestern expansion of the United States in the 1800s and caused a loss of 5% in total annual runoff. *Deems et al.* [2013a] expanded this analysis by using the dust conditions present in the years 2009 and 2010, 2 years of much greater dust loading, and showed snowmelt 6 weeks earlier than predisturbance dust loading and a 6% loss in total runoff. It is problematic therefore, that streamflow prediction in the UCRB does not explicitly include dust deposition.

1.6 Research Questions and Methods

Radiative forcing by dust in snow has been measured using two micrometeorology towers in southwestern, CO since 2003 [*Painter et al.*, 2012] and ground based measurements of dusty-snow spectral reflectance have been taken at multiple locations throughout the UCRB with an Analytical Spectral Devices field-portable spectroradiometer over the same period. However, all of these data speak to dust radiative forcing at a discrete location, representative of a limited spatial extent. Spatially comprehensive measurements of dust radiative forcing are lacking, inhibiting our ability to monitor and quantify hydrologic impacts throughout the basin.

Therefore, to address this knowledge gap in our understanding of the Colorado River system, the following research questions are posed: 1) Can we use Moderate Resolution Imaging Spectroradiometer (MODIS) remote sensing data and in situ data to infer the approximate radiative forcings from dust on snow; 2) What are the spatial and temporal patterns of radiative forcing inferred from MODIS retrievals across the UCRB; and 3) Is dust radiative forcing over the rising limb of the hydrograph correlated to snowmelt prediction errors in the UCRB?

In short, the purpose of this dissertation is to advance our knowledge and understanding of the spatial and temporal variability of dust radiative forcing in snow across the UCRB using remote sensing to provide spatially comprehensive measurements of dust radiative forcing in snow and, ultimately, use those data to understand how the spatial and temporal variability of dust on snow impacts operational streamflow prediction.

1.6.1 Remote sensing

Remote sensing can provide spatially comprehensive data to estimate dynamics of the terrestrial system. The goal of optical remote sensing of snow is to infer the physical properties of snow based on a given spectral response. Multispectral sensors such as the MODIS have enabled the analysis of snow properties because its radiometric range in the VIS does not saturate at the large radiances from snow, daily global coverage, and nominal 500 m pixel resolution. Other multispectral sensors such as the pre-Landsat-8 Thematic Mappers and the NASA Advanced Spaceborne Thermal Emission and Reflection Radiometer (ASTER) saturate at reflectances usually less than 50% in the

VIS, precluding their use to estimate the radiative impacts of dust on snow. Fortunately, the location and dynamic range of MODIS band passes enables the detection of changes in absorption in the VIS, attributed to dust, and changes in grain size expressed in the NIR/SWIR. Therefore, we can use MODIS data to infer radiative forcing by dust in snow over the UCRB and use radiative forcing retrievals from two energy balance towers in the Senator Beck Basin Study Area for validation.

1.6.2 Streamflow prediction

The Colorado Basin River Forecast Center (CBRFC) produces operational streamflow forecasts using the coupled SNOW-17 temperature-index based model [*Anderson*, 1976] and Sacramento Soil Moisture Accounting (Sac-SMA) [*Burnash et al., 1973*] model. Temperature-index models, such as SNOW-17, provide a powerful technique for measuring snowmelt at basin to regional scales when the assumption of a linear relationship between temperature and snowmelt persists. We hypothesize, however, that the perturbation of snowpack energy balance attributed to dust deposition will introduce error into SNOW-17 snowmelt predictions.

1.7 Research Contributions

The results of this research are presented in three chapters formatted as journal articles. Chapters 2 and 3 have been published, while Chapter 4 is in preparation for publication. Chapter 2 presents the MODIS Dust Radiative Forcing in Snow (MODDRFS) model, which retrieves surface radiative forcing by dust in snow from Moderate Resolution Imaging Spectroradiometer (MODIS) surface reflectance data. The MODDRFS retrieval reduces a critical void in our knowledge of the spatial and temporal

variations of radiative forcing by dust on snow around the UCRB. Further, because MODDRFS retrievals span the majority of snow-covered regions around the world, these data provide scientists, policy makers, and resource managers with a tool to better understand how radiative forcing by dust impacts glacier mass balance, regional hydrology, and climate on a global scale.

Chapter 3 explores the sensitivity of streamflow prediction errors to dust radiative forcing between years 2000 and 2010, as inferred by the MODDRFS remote sensing product (described in Chapter 2) in four headwater catchments in southwestern Colorado. This chapter shows that interannual variability of dust radiative forcing is correlated to the prediction accuracy of the temperature index-based SNOW-17 snowmelt model used by the Colorado Basin River Forecast Center (CBRFC). Further, in the move towards more physically-based snowmelt models that will eventually be used by all US River Forecast Centers, the results in Chapter 3 suggest that MODDRFS could constrain energy balance components relative to dust on snow.

Chapter 4 expands on Chapter 3, by comparing interannual variability of dust radiative forcing to streamflow prediction errors in 11 basins that span the UCRB. In addition, Chapter 4 presents annual maps of maximum dust radiative forcing across the UCRB that suggest the spatial variability of dust forcing is driven by both proximity and orientation to dust emission sources in the Colorado Plateau. These results highlight the need to explicitly treat the spatial and temporal heterogeneity of dust radiative forcing in the UCRB when modeling basin-wide hydrologic impacts of dust on snow. Further, Chapter 4 shows that MODDRFS retrievals can reduce uncertainties in the SNOW-17

modeled streamflow, reducing the strain on those tasked with monitoring the Colorado River system over a period of growing demand and climatic uncertainty.

Lastly, this combined body of work provides new methods, tools, and insights that are relevant for a broad range of scientific inquiry. Adaptation of the methods presented herein to future satellite retrievals will likely enable further lines of inquiry and an increased capacity to integrate dust radiative forcing data into operational streamflow prediction.

1.8 References

Anderson, E. A. (1976), A point energy and mass balance model of a snow cover, *NOAA Tech. Rep. NWS, Natl. Oceanic and Atmos. Admin., Silver Spring, Md.*, *19*.

Bales, R. C., N. P. Molotch, T. H. Painter, M. D. Dettinger, R. Rice, and J. Dozier (2006), Mountain hydrology of the western United States, *Water Resources Research*, *42*.

Barnett, T. P. and D. W. Pierce (2009), Sustainable water deliveries from the Colorado River in a changing climate, *P. Natl. Acad. Sci.*, *106*, 7334-7338, doi: 10.1073/pnas.0812762106.

Barnett, T. P., D. W. Pierce, H. G. Hidalgo, C. Bonfils, B. D. Santer, T. Das, G. Bala, A. W. Wood, T. Nozawa, A. A. Mirin, D. R. Cayan, and M. D. Dettinger (2008), Human-induced changes in the hydrology of the western United States, *Science*, *319*, 1080-1083, doi: 10.1126/science.1152538.

Brahney, J., A. P. Ballantyne, C. Sievers, and J. C. Neff (2013), Increasing Ca 2+ deposition in the western US: The role of mineral aerosols, *Aeolian Research*, doi: 10.1016/j.aeolia.2013.04.003.

Burnash, R. J., R. L. Ferral, and R. A. McGuire (1973), A Generalized Streamflow Simulation System Conceptual Modeling for Digital Computers, *U.S. Department of Commerce National Weather Service and State of California Department of Water Resources,* Report by the Joliet Federal State River Forecasts Center, Sacramento, CA.

Cayan, D. R. (1996), Interannual climate variability and snowpack in the western United States, *Journal of Climate*, *9*, 928-948.

Christensen, N. S., A. W. Wood, D. P. Lettenmaier, and R. N. Palmer (2004), Effects of climate change on the hydrology and water resources of the Colorado River Basin, *Journal of Hydroclimatology*, *62*, 337-363, doi: 10.1023/B:CLIM.0000013684.13621.1f.

Conway, H., A. Gades, and C. F. Raymond (1996), Albedo of dirty snow during conditions of melt, *Water Resources Research*, *32*, 1713-1718.

Center for Snow and Avalanche Studies (2013), *Archival Data from Senator Beck Basin Study Area.* http://www.snowstudies.org/.

Deems, J. S., T. H. Painter, J. J. Barsugli, J. Belnap, and B. Udall (2013a), Combined impacts of current and future dust deposition and regional warming on Colorado River Basin snow dynamics and hydrology, *Hydrol. Earth Syst. Sc. Disc.*, *10*, 6237-6275, doi: 10.5194/hessd-10-6237-2013.

Deems, J. S., T. H. Painter, and D. C. Finnegan (2013b), Lidar measurement of snow depth: a review, *Journal of Glaciology*, *59*, 467.

Dozier, J., R. E. Davis, A. T. C. Chang, and K. Brown (1988), The spectral bidirectional reflectance of snow, *4th International Colloquium on Spectral Signatures of Objects in Remote Sensing*, vol., pp. 87-92, Aussois, France.

Draut, A. E., M. Hiza Redsteer, and L. Amoroso (2012), Recent seasonal variations in arid landscape cover and aeolian sand mobility, Navajo Nation, southwestern United States, *Geophysical Monograph Series*, *198*, 51-60.

Fassnacht, S. R., K. A. Dressler, and R. C. Bales (2003), Snow water equivalent interpolation for the Colorado River Basin from snow telemetry (SNOTEL) data, *Water Resources Research*, *39*, doi:10.1029/2002WR001512.

Franz, K. J., T. S. Hogue, and S. Sorooshian (2008), Operational snow modeling: Addressing the challenges of an energy balance model for National Weather Service forecasts, *J. Hydrol.*, *360*, 48-66, doi: 10.1016/j.jhydrol.2008.07.013.

Hansen, J., and L. Nazarenko (2004), Soot climate forcing via snow and ice albedos, *P. Natl. Acad. Sci.*, *101*, 423-428, doi: 10.1073/pnas.2237157100.

Kaspari, S. D., M. Schwikowski, M. Gysel, M. G. Flanner, S. Kang, S. Hou, and P. A. Mayewski (2009), Recent increase in black carbon concentrations from a Mt. Everest ice core spanning 1860,Äì2000 AD, *Geophysical Research Letters*, *38*.

Marks, D., and A. Winstral (2001), Comparison of snow deposition, the snow cover energy balance, and snowmelt at two sites in a semiarid mountain basin, *Journal of Hydrometeorology*, *2*, 213-227.

McConnell, J. R., R. Edwards, G. L. Kok, M. G. Flanner, C. S. Zender, E. S. Saltzman, J. R. Banta, D. R. Pasteris, M. M. Carter, and J. D. W. Kahl (2007), 20th-century industrial black carbon emissions altered Arctic climate forcing, *Science*, *317*, 1381-1384.

Molotch, N. P., and S. A. Margulis (2008), Estimating the distribution of snow water equivalent using remotely sensed snow cover data and a spatially distributed snowmelt model: A multi-resolution, multi-sensor comparison, *Advances in Water Resources*, *31*, 1503-1514, doi: 10.1016/j.advwatres.2008.07.017.

Mote, P. W., A. F. Hamlet, M. P. Clark, and D. P. Lettenmaier (2005), Declining mountain snowpack in western North America, *Bulletin of the American Meteorological Society*, *86*, 39-49, doi: 10.1175/BAMS-86-1-39.

Neff, J. C., A. P. Ballantyne, G. L. Farmer, N. M. Mahowald, J. L. Conroy, C. C. Landry, J. T. Overpeck, T. H. Painter, C. R. Lawrence, and R. L. Reynolds (2008), Increasing eolian dust deposition in the western United States linked to human activity, *Nat. Geosci.*, doi: 10.1038/ngeo133.

Painter, T. H., A. P. Barrett, C. C. Landry, J. C. Neff, M. P. Cassidy, C. R. Lawrence, K. E. McBride, and G. L. Farmer (2007), Impact of disturbed desert soils on duration of mountain snow cover, *Geophys. Res. Lett.*, *34*, doi: 10.1029/2007GL030284.

Painter, T. H., J. S. Deems, J. Belnap, A. F. Hamlet, C. C. Landry, and B. Udall (2010), Response of Colorado River runoff to dust radiative forcing in snow, *P. Natl. Acad. Sci.*, *107*, 17125-17130, doi: 10.1073/pnas.0913139107.

Painter, T. H., S. Skiles, J. Deems, C. Landry, and A. Bryant (2012), Dust radiative forcing in snow of the Upper Colorado River Basin: Part I. A 6 year record of energy balance, radiation, and dust concentrations, *Water Resour. Res.*, *48*, doi: 10.1029/2012WR011985.

Pierce, D. W., T. P. Barnett, H. G. Hidalgo, T. Das, C. Bonfils, B. D. Santer, G. Bala, M. D. Dettinger, D. R. Cayan, A. Mirin, A. W. Wood, and T. Nozawa (2008), Attribution of declining western U.S. snowpack to human effects, *Journal of Climate*, *21*, 6425-6444, doi: 10.1175/2008JCLI2405.1.

Rice, R., R. C. Bales, T. H. Painter, and J. Dozier (2011), Snow water equivalent along elevation gradients in the Merced and Tuolumne River basins of the Sierra Nevada, *Water Resources Research*, *47*, W08515.

Skiles, S. M., T. H. Painter, J. S. Deems, A. C. Bryant, and C. C. Landry (2012), Dust radiative forcing in snow of the Upper Colorado River Basin: Part II. Interannual variability in radiative forcing and snowmelt rates, *Water Resour. Res.*, doi: 10.1029/2012WR011986.

Thompson, L. G., T. Yao, E. Mosley-Thompson, M. E. Davis, K. A. Henderson, and P.-N. Lin (2000), A high-resolution millennial record o the south Asian monsoon from Himalayan ice cores, *Science*, *289*, 1916-1919.

U.S. Dept. of Int., B. o. R. (2013), Colorado River Basin Water Supply and Demand Study, Interim Report No. 1, Technical Report B – Water Supply Assessment, Bureau of Reclamation, US Department of the Interior.

Vano, J. A., T. Das, and D. P. Lettenmaier (2012), Hydrologic sensitivities of Colorado River runoff to changes in precipitation and temperature, *Journal of Hydrometeorology*, *13*, 932-949.

Warren, S. G. (1982), Optical properties of snow, *Reviews of Geophysics and Space Physics*, *20*, 67-89.

Wiscombe, W. J., and S. G. Warren (1980), A model for the spectral albedo of snow, I, Pure snow, *Journal of the Atmospheric Sciences*, *37*, 2712-2733.

CHAPTER 2[1]

RADIATIVE FORCING BY LIGHT ABSORBING IMPURITIES IN SNOW FROM MODIS SURFACE REFLECTANCE DATA

[1] Reprinted with permission of American Geophysical Union. Painter, T. H., A. C. Bryant, and S. M. Skiles (2012), Radiative forcing by light absorbing impurities in snow from MODIS surface reflectance data, *Geophys. Res. Lett.*, *39*, L17502, doi: 10.1029/2012gl052457.

GEOPHYSICAL RESEARCH LETTERS, VOL. 39, L17502, doi:10.1029/2012GL052457, 2012

Radiative forcing by light absorbing impurities in snow from MODIS surface reflectance data

Thomas H. Painter,[1] Ann C. Bryant,[2] and S. McKenzie Skiles[3]

Received 18 June 2012; revised 18 July 2012; accepted 23 July 2012; published 11 September 2012.

[1] The episodic deposition of dust and carbonaceous particles to snow decreases snow surface albedo and enhances absorption of solar radiation, leading to accelerated snowmelt, negative glacier mass balance, and the snow-albedo feedback. Until now, no remote sensing retrieval has captured the spatial and temporal variability of this forcing. Here we present the MODIS Dust Radiative Forcing in Snow (MODDRFS) model that retrieves surface radiative forcing by light absorbing impurities in snow cover from Moderate Resolution Imaging Spectroradiometer (MODIS) surface reflectance data. Validation of MODDRFS with a 7-year record of in situ measurements indicates the radiative forcing retrieval has positive bias at lower values and slight negative bias above 200 W m^{-2}, subject to mixed pixel uncertainties. With bias-correction, MODDRFS has a root mean squared error of 32 W m^{-2} and mean absolute error of 25 W m^{-2}. We demonstrate MODDRFS in the Upper Colorado River Basin and Hindu Kush-Himalaya.
Citation: Painter, T. H., A. C. Bryant, and S. M. Skiles (2012), Radiative forcing by light absorbing impurities in snow from MODIS surface reflectance data, *Geophys. Res. Lett.*, *39*, L17502, doi:10.1029/2012GL052457.

1. Introduction

[2] Mountain snowmelt dominates the fresh water supply to more than 1/6 of Earth's human population [*Barnett et al.*, 2005]. While much effort has been spent on understanding the impacts of anthropogenic climate change on snowmelt [*Howat and Tulaczyk*, 2005; *Mote et al.*, 2005], recent in situ observations and modeling show that surface radiative forcing of snow and glacier melt by light absorbing impurities (LAI) such as dust and carbonaceous particles also markedly accelerates snowmelt and modifies regional water cycles [*Hansen and Nazarenko*, 2004; *Painter et al.*, 2007; *Flanner et al.*, 2009; *Qian et al.*, 2009; *Painter et al.*, 2010].

[3] In the Upper Colorado River Basin, USA, detailed energy balance and radiation measurements show that surface radiative forcing by desert dust from the Colorado Plateau shortens snow cover duration by 25–50 days [*Painter et al.*, 2007; *Skiles et al.*, 2012]. Dust loading there has increased five to seven-fold since the Anglo-settlement of the western US in the mid-1800s [*Neff et al.*, 2008]. Extrapolating these point measurements to the entire upper basin suggests that this increase in dust loading and reduction in snow albedo from the earlier background load has brought peak runoff three weeks earlier and caused a loss of 5% in total annual runoff [*Painter et al.*, 2010].

[4] Growing point observations and modeling simulations also suggest that increasing LAI deposition to snow in the Hindu Kush-Himalaya may be leading to accelerated snowmelt and glacier retreat [*Ramanathan et al.*, 2007; *Kaspari et al.*, 2009]. In the eastern Himalaya, dust loading to mountain snow increased four-fold since the mid 19th century [*Thompson et al.*, 2000] and black carbon loading to snow increased three-fold since the 1970s [*Kaspari et al.*, 2011]. These results, along with studies of the damaging health impacts of black carbon and other industrial pollutants, have led to recent calls for reductions in emissions from the *United Nations Environmental Programme* [2011] and the US Department of State's initiation of the Climate and Clean Air Coalition to Reduce Short-Lived Climate Pollutants. However, all of these studies of radiative impacts of LAI in snow or ice have derived from or been constrained by starkly limited in situ measurements because we have lacked remote sensing measurements of radiative forcing by LAI in snow and installation and maintenance of in situ infrastructure is extremely difficult in these harsh and dangerous environments. To address this void in our knowledge, we have developed the MODIS Dust Radiative Forcing in Snow (MODDRFS) model to retrieve radiative forcing by LAI in snow cover.

2. Background

[5] Snow without absorbing impurities has the highest albedo of any naturally occurring Earth surface. The spectral albedo of pure snow (α_{pure}) is sensitive to changes in snow optical grain radius (OGR) and the solar zenith angle for direct beam solar radiation (Figure 1). As grain size increases, spectral albedo drops primarily in the near infrared and shortwave infrared where the imaginary part of the complex index of refraction for ice is orders of magnitude greater than in the visible portion [*Wiscombe and Warren*, 1980]. As solar zenith angle increases, forward single scattering becomes more dominant thus increasing spectral albedo.

[6] When impurities such as dust or carbonaceous particles are present however, snow albedo decreases primarily in the visible wavelengths (VIS) with the reduction occurring at longer wavelengths as concentration and/or absorption increases (Figure 1c) [*Singh et al.*, 2010; *Brandt et al.*, 2011]. This albedo drop results from the contrast of the imaginary part of the complex refractive index for the light absorbing

[1]Jet Propulsion Laboratory, California Institute of Technology, Pasadena, California, USA.
[2]Department of Geography, University of Utah, Salt Lake City, Utah, USA.
[3]Department of Geography, University of California, Los Angeles, California, USA.

Corresponding author: T. H. Painter, Jet Propulsion Laboratory, California Institute of Technology, M/S 233-306D, 4800 Oak Grove Dr., Pasadena, CA 91109, USA. (thomas.painter@jpl.nasa.gov)

0094-8276/12/2012GL052457

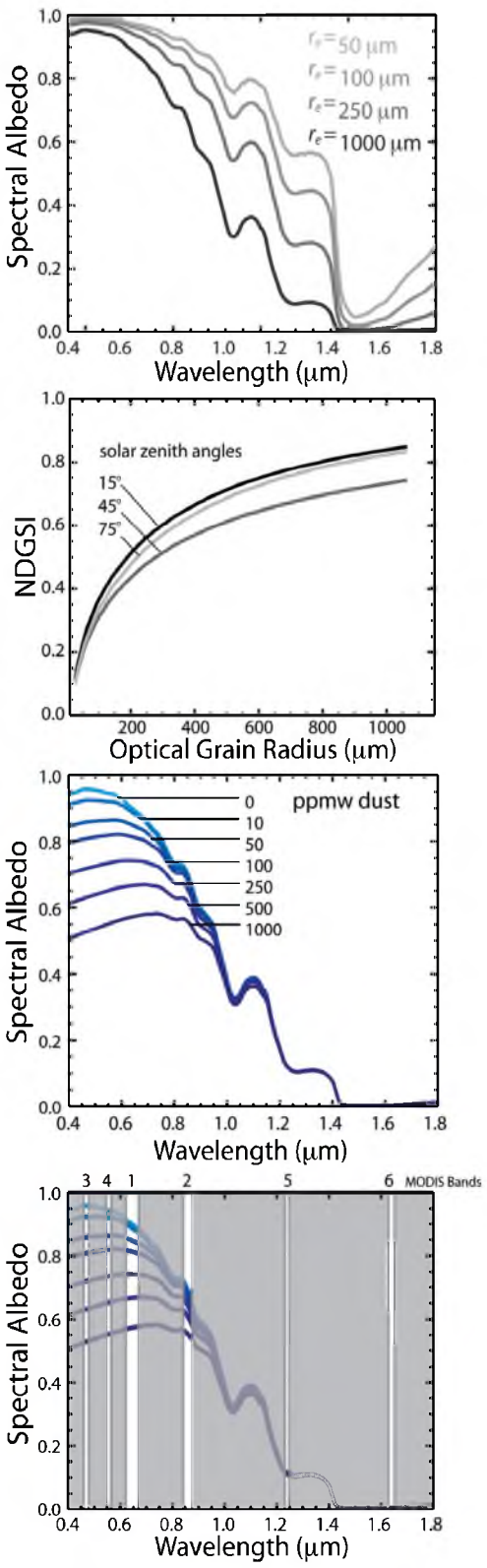

particles with that of the highly transparent ice [*Warren and Wiscombe*, 1980]. Our experience suggests that the aeolian deposition of LAI to snow does not accumulate to the degree that the spectral reflectance of the surface shifts from snow to soil (see *Skiles et al.* [2012] for LAI concentrations in the UCRB). We hypothesize (but do not test here) that such a shift occurs only from rock fall or in glacier moraines from glacial transport.

[7] Radiative forcing by LAI in snow is considered in terms of its direct effect and two feedbacks [*Hansen and Nazarenko*, 2004], with further definition of at-surface or at-tropopause. In this work, we retrieve at-surface radiative forcing. The direct effect comes from the enhanced absorption of solar irradiance by the LAI themselves, primarily in the VIS and NIR. The first feedback comes from the enhanced absorption by larger grain size due to accelerated snow grain growth driven by the direct effect. This affects the entire spectrum by reinforcing the direct absorption in the VIS and increasing the absorption in the NIR through shortwave infrared by the larger absorbing path length. Finally, the second feedback comes from the enhanced absorption of solar irradiance by the usually darker substrate (i.e. soil, rock, and/or vegetation), exposed earlier due to the direct and first feedback.

[8] Radiative forcing by LAI in snow and the ability to quantify it with optical remote sensing come from two physical properties: (i) larger particles (greater than ~5.0 μm) tend to accumulate near the snow surface as ablation advances [*Conway et al.*, 1996], and (ii) transported LAI arrive and concentrate during late winter and spring when solar irradiance is increasing and most of the seasonal snow accumulation has occurred [*Wake and Mayewski*, 1994; *Kaspari et al.*, 2009]. The LAI therefore often lie near the surface where they can absorb solar radiation and immediately conduct that energy to surrounding snow grains [*Painter et al.*, 2012].

3. Data and Methods

[9] MODIS data have enabled the analysis of snow properties beyond snow covered area (SCA) because its radiometric range in the VIS does not saturate at the large radiances from snow. Other multi-spectral sensors such as the pre-Landsat-8 Thematic Mappers and the NASA Advanced Spaceborne Thermal Emission and Reflection Radiometer (ASTER) saturate at reflectances usually less than 50% in the VIS, leaving the impact of LAI unknowable. Fortunately, the dynamic range in the VIS bands of the Operational Line Imager (OLI) on Landsat-8 should not saturate over snow, thereby enabling frequent rigorous validation of the MODDRFS product. The location and dynamic range of MODIS band passes enables the detection of changes in absorption in the VIS and changes in grain size expressed in the NIR/SWIR (Figure 1d).

3.1. MODDRFS

[10] The MODDRFS algorithm infers per-pixel radiative forcing by LAI in snow using MODIS surface reflectance

Figure 1. (a) Snow albedo variation with grain size. (b) NDGSI for MODIS data with sensitivity to solar zenith angle. (c) Snow albedo variation with dust concentration. (d) Same as Figure 1c, but with MODIS bandpasses indicated in transparent wavelengths and parts of spectrum not sampled by black-obscured wavelengths.

data (Terra MODIS MOD09GA, Aqua MODIS MYD09GA; we speak to MOD09GA only for brevity) and a coupled radiative transfer model for snow. MODDRFS determines the spectral reflectance differences between the measured MODIS spectrum and the modeled clean snow spectrum of the same OGR. Integration of the band-wise multiplication of this spectral difference with local spectral irradiance that accounts for terrain variations gives the instantaneous at-surface radiative forcing (W m^{-2}).

[11] MODDRFS first determines those pixels that can provide more robust retrievals (relatively free of mixing) from the MODIS Snow Covered Area and Grainsize (MODSCAG) fractional snow and vegetation products [*Painter et al.*, 2009]. MODSCAG finds maximal snow cover in winter/spring from a time series approach, from which we determine the per-pixel potential for complete cover. Among those pixels, we then use each acquisition's retrievals of fractional vegetation to remove those pixels that have a mixed cover of vegetation that has been exposed since maximum cover. We do not take this step for the mixed cover of rock because it would be confused with and remove pixels impacted by LAI (which introduces error - section 5.2 below).

[12] As with the spectral albedo of snow, the spectral hemispherical-directional reflectance factor (HDRF [*Schaepman-Strub et al.*, 2006] – the MOD09GA retrieval) of snow also varies with grain size (Figure 1). We estimate the OGR and identify the clean snow HDRF through the normalized difference grain size index (NDGSI):

$$NDGSI = \left(\frac{MODIS_2 - MODIS_5}{MODIS_2 + MODIS_5}\right) \quad (1)$$

where $MODIS_2$ is the MOD09GA surface reflectance in MODIS band 2 (band center ~0.858 μm) and $MODIS_5$ is the MOD09GA surface reflectance in MODIS band 5 (band center ~1.240 μm) (Figure 1d). NDGSI has a logarithmic relationship with OGR due to the decreasing changes in HDRF with increases in OGR, and is sensitive to solar zenith angle (SZA) (Figure 1b). From the OGR, we determine the clean snow spectrum for the same OGR and SZA with the discrete ordinates solution to the radiative transfer equation. The description of these clean snow spectra is given in the auxiliary material.[1]

[13] We use the Santa Barbara DISORT Atmospheric Radiative Transfer (SBDART) model in conjunction with the 3 arc second Shuttle Radar Topography Mission (SRTM) digital elevation model (DEM) to estimate per-pixel clear sky incident spectral irradiance. The University of Wisconsin's MODIS Terra overpass predictor (http://eosweb.ssec.wisc.edu/) was used to determine the time of acquisition and solar ephemeris. Direct and diffuse spectral irradiance are first modeled in SBDART for a range of SZA and elevation bands. Incident spectral irradiances are then determined at 1/5th MODIS pixel spatial resolution and up-scaled to obtain the mean per-MODIS pixel irradiance spectrum. Per-pixel terrain slope and aspect give the plane to which we correct the direct component of level-surface solar irradiance according to the following relationship:

$$\cos\beta = \cos\theta_s \cos\theta_n + \sin\theta_s \sin\theta_n \cos\{\phi_s - \phi_n\} \quad (2)$$

[1]Auxiliary materials are available in the HTML. doi:10.1029/2012GL052457.

where β is the local solar zenith angle, θ_s is the solar zenith angle for a level surface, ϕ_s is the solar azimuth angle, θ_n is the surface slope, and ϕ_n is the surface aspect. We then determine corrected per-pixel solar spectral irradiances, $E_{corrected,\lambda}$, according to:

$$E_{corrected,\lambda} = \left(E_{direct,\lambda} \cos\beta\right) + E_{diffuse,\lambda} \quad (3)$$

where E_{direct} and $E_{diffuse}$ are the direct and diffuse spectral irradiances. This calculation assumes that the diffuse and terrain-scattered irradiances are identical. It is valid to first order and ameliorates the need for a complex, intensive topographic treatment for this global product.

[14] Because MODIS does not measure the entire hemisphere-reflected flux, we must use the modeled understanding of the relationship between the MODIS-derived spectral HDRF and hemispherical spectral albedos [*Schaepman-Strub et al.*, 2006]. Here we use scalars, c, between the directional reflectance spectrum at the observation geometry, R, and the spectral albedo for the same irradiance geometry:

$$\alpha_{clean,\lambda} = c(\lambda; \theta_0; \theta_r, \phi_r; \zeta_{atm}) \cdot R(\lambda; \theta_0; \theta_r, \phi_r; \zeta_{atm}) \quad (4)$$

where λ denotes the wavelength, θ_0 and θ_r the solar and viewing zenith angles, ϕ_r the relative azimuth and ζ_{atm} the atmospheric properties.

[15] Because of the lack of spectral continuity in the MODIS spectrum we do not know the wavelength at which the measured and modeled clean spectra diverge (Figure 1c). To account for this, the measured spectrum is fit to the clean spectrum at $MODIS_2$ (band center wavelength ~0.858 μm and upper end ~0.876 μm) and we determine the radiative forcing for the wavelength range down to 0.35 μm. Moreover, because of the discrete bands, we model the irradiances and spline albedos to a continuous spectrum of 0.01 μm bands across the range 0.350–0.876 μm. We then retrieve the radiative forcing estimate, F, from the following:

$$F = \sum_{\lambda=0.35\mu m}^{\lambda=0.876\mu m} E_{corrected,\lambda}\left(\alpha_{clean,\lambda} - \alpha_{MODIS,\lambda}\right)\Delta\lambda \quad (5)$$

where $E_{corrected, \lambda}$ is the corrected irradiance, $\alpha_{clean, \lambda}$ is the clean snow spectral albedo of the MODIS OGR, $\alpha_{MODIS, \lambda}$ is the spectral albedo of the MODIS pixel, and $\Delta\lambda$ is 0.01 μm. The retrieved radiative forcings are then instantaneous values and not daily averages convolved with the diurnal cycle of irradiances.

4. Validation

[16] Validation of MODDRFS, and any other future remote sensing retrievals of surface radiative forcing by LAI, is limited by a relative paucity of in situ data. The only in situ temporally extensive measurements of radiative forcing by LAI of which we are aware come from the Western Energy Balance of Snow (WEBS) network of energy balance and radiation towers operated by collaborators and the lead author in the Colorado River Basin. This network consists of heavily instrumented towers in snow-covered regions to facilitate modeling of the energy balance and melt of snow cover, and LAI radiative forcing in the snow cover. These unique measurements have provided important insights into

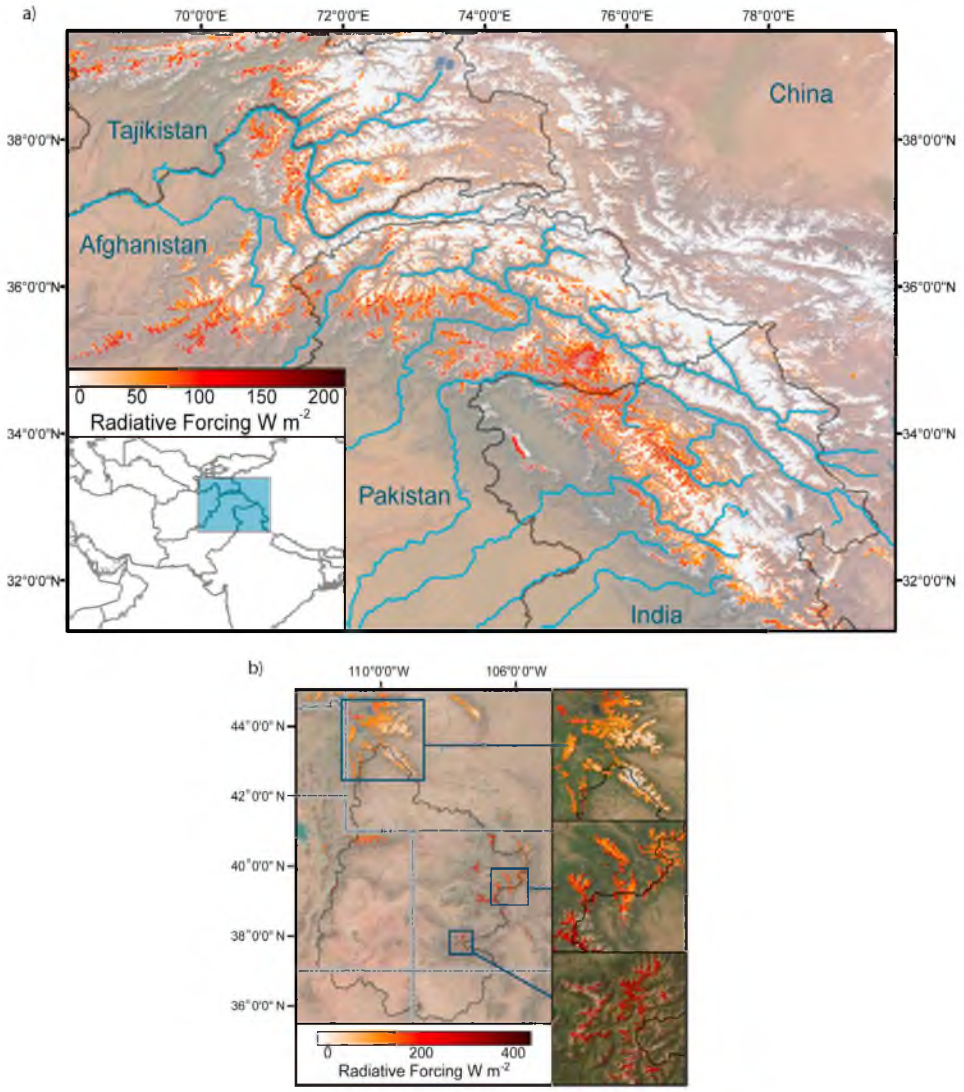

Figure 2. (a) Dust radiative forcing in snow for Hindu Kush-Himalaya on 21 June 2010 at time of MODIS overpass, ~05:40 UTC. (b) Dust radiative forcing in snow for eastern half of the Upper Colorado River Basin on 18 May 2009 at time of MODIS overpass, ~17:55 UTC.

the controls on snowmelt by LAI radiative forcing [*Painter et al.*, 2007] and their impact on runoff timing and loss of volume [*Painter et al.*, 2010, 2012; *Skiles et al.*, 2012].

[17] We validate the instantaneous MODDRFS against the coincident in situ surface radiative forcing data from two WEBS stations (alpine and subalpine) in the Senator Beck Basin Study Area (SBBSA), San Juan Mountains in the Upper Colorado River Basin (37° 54′ 30″ N, 107° 43′ 30″ W). In addition to standard measurements of meteorology (air temperature, wind speed, relative humidity, all at two heights), the towers measure incident and reflected broadband solar radiation and incident and reflected NIR/SWIR solar radiation [*Painter et al.*, 2012]. From the radiation measurements, we determine hourly LAI radiative forcing from the relationships described in *Painter et al.* [2007]. We choose the coincident in situ hourly data in which the MODIS acquisition falls.

[18] We assess only MODDRFS/MODIS data with sensor zenith angles <30° over the alpine and sub-alpine energy balance towers in SBBSA. At larger sensor zenith angles, the ground instantaneous field of view expands well beyond that at nadir and spatial mixing becomes severe [*Dozier et al.*, 2008], rendering the MODDRFS retrieval unreliable. The spectral range that MODDRFS infers surface radiative forcing (0.350–0.876 μm) does not perfectly align with that of the energy balance towers (0.305–0.780 μm). Part of the MODDRFS error described below comes from this difference.

5. Results

[19] We show MODDRFS for the Hindu Kush-Himalaya (HKH) in Asia on 21 June 2010 (Figures 2a and S1a) and the

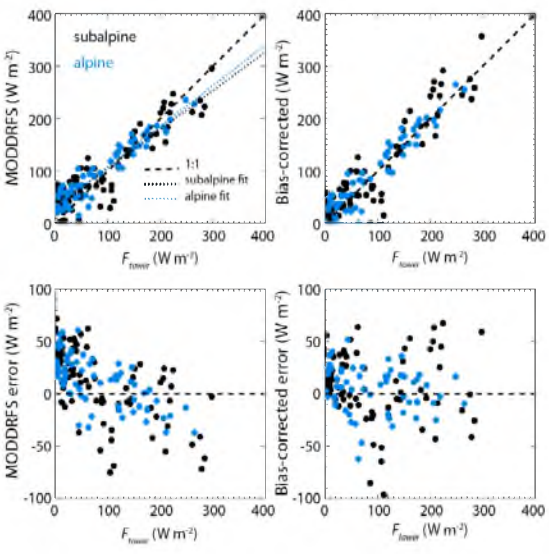

Figure 3. Validation of MODDRFS retrieved F with in situ estimated F from Swamp Angel Study Plot and Senator Beck Study Plot, Colorado across 2005 through 2011.

Upper Colorado River Basin, USA on 18 May 2009 (Figures 2b and S1b). These example retrievals indicate that gradients occur in radiative forcing across regional and finer scales.

[20] In the HKH, south and western ranges have higher forcings reaching >200 W m^{-2}, most likely due to their exposure to transport of LAI from the deserts of the Middle East, Asia and North Africa, and industrial regions in Pakistan and India (Figure 2a). Within individual ranges, the most distinctive gradient is the decrease in forcing with increasing elevation. However, it is important to note that MODIS only provides the capacity to retrieve a daily snapshot of forcing. As snowmelt advances, dust layers may emerge at higher elevations and affect similar radiative forcings to those observed earlier at lower elevations.

[21] In the Upper Colorado River Basin, regional gradients are also revealed with variations that are likewise sensitive to the mountain proximity to sources of LAI. In the southern box in Figure 2 (San Juan Mountains, CO), closest to the dust source regions of the Colorado Plateau, radiative forcing by LAI is relatively constant across the domain with a mean forcing of ~250 W m^{-2}. In the central box (Elk Range to Front Range, CO), greater spatial variability is expressed with a range of forcings from 250 W m^{-2} in the southwest to ~100 W m^{-2} in the northeast, most remote from the dust source regions. The northwest part of the Upper Colorado shows the most pronounced spatial variation. From the 30 70 W m^{-2} in the Wind River range in the southeast part of this subregion to 200 W m^{-2} in the plateaus west of Yellowstone Lake in the northwest part. This latter region is downwind of dust producing regions of the Snake River Plain, Idaho.

[22] Figure 3 shows the validation of MODDRFS based on data from 2005–2011. At the subalpine site, the root mean squared error (RMSE) for MODDRFS against F_{tower} was 39 W m^{-2}, with mean absolute error (MAE) of 22 W m^{-2}, and mean error of +8 W m^{-2}. The errors show a positive MODDRFS bias at lower F_{tower} casing to a smaller magnitude negative bias at higher F_{tower}. The linear least squares fit of MODDRFS and F data is MODDRFS = β_1 F_{tower} − β_0, where β_1 = 0.72 ± 0.15 (95% confidence interval) and β_0 = 31.9 ± 19.3 with an R^2 of 0.83. To 95% confidence, β_1 and β_0 are different from 1.0 and 0.0, respectively.

[23] At the alpine site, the RMSE for MODDRFS against F_{tower} was 36 W m^{-2}, with a MAE of 26 W m^{-2}, and mean error of +7 W m^{-2}. As with the subalpine site, MODDRFS overestimates radiative forcing at lower F_{tower} and slightly underestimates at the higher F_{tower}. The least squares fit to the MODDRFS and F_{tower} data has β_1 = 0.67 ± 0.17 and β_0 = 36.9 ± 21.1 with an R^2 of 0.86. Again, to 95% confidence, β_1 and β_0 are different from 1.0 and 0.0, respectively.

[24] For these data combined, the linear least squares regression has RMSE of 33 W m^{-2}, with a MAE of 28 W m^{-2}, and mean error of 10 W m^{-2}. The regression yields coefficients of β_1 = 0.75 ± 0.11 and β_0 = 31.2 ± 14.4 with an R^2 of 0.86 (Figure 3). In all cases, MODDRFS has a positive bias at lower F_{tower} and slightly negative bias at higher F_{tower}.

5.1. Bias Correction

[25] The assessments of MODDRFS at the sub-alpine and alpine towers are consistent in magnitude of errors and in their biased relationships within the uncertainties of 95% confidence intervals (Figure 3). Given the relatively high R^2, we can assess a correction of the bias to provide more robust results calibrated from the towers. We force the fit to a slope of 1.0 and intercept of 0.0 based on the energy balance data. We fully recognize that this relationship is specific to the WEBS towers in the San Juan Mountains, USA, and is thus regionally specific. Nevertheless, these are the only viable measurements globally for such purpose and thus we proceed cautiously. The final bias-corrected MODDRFS retrieval is:

$$F_{biascorr} = \frac{\left(\left(\sum_{\lambda=0.35\mu m}^{\lambda=0.876\mu m} E_{corrected,\lambda}\left(\alpha_{clean,\lambda} - \alpha_{MODIS,\lambda}\right)\Delta\lambda\right) - 31.20\right)}{0.75} \quad (6)$$

The RMSE for the bias-corrected MODDRFS retrievals is 32 W m^{-2}, MAE is 25 W m^{-2}, but by definition the mean error is 0.0 W m^{-2}. Taken piecewise, errors in raw and bias-corrected MODDRFS retrievals are both sensitive to magnitude of forcing (Figure 3). For the radiative forcing range 0–100 W m^{-2} at the towers, the RMSE for uncorrected MODDRFS is 37 W m^{-2} and for bias-corrected is 29 W m^{-2}. In the range 100–200 W m^{-2}, the RMSE for uncorrected and bias-corrected are 23 and 24 W m^{-2}, respectively. The errors rise again in the range 200–300 W m^{-2} to 38 and 34 W m^{-2}, respectively. Note that the MODDRFS algorithm determines radiative forcing whereas it is not designed to invert for LAI concentration. However, subsequent work can use assumptions of the spectral complex refractive index of the LAI to invert the MODDRFS retrievals for an effective concentration. These retrievals will be highly uncertain however.

5.2. Uncertainties

[26] Uncertainties in the MODDRFS retrieval are driven by the sensor properties, atmospheric correction, snow

geographic and geomorphological properties, and subpixel terrain heterogeneity. The discrete and variably spaced bands of MODIS prevent continuous measurement of a continuously variable forcing like that which LAI impart to snow albedo. Therefore, this retrieval is semi-quantitative whereas a spectrometer with contiguous bands across the spectrum allows the more quantitative retrieval. The uncertainty of the retrieval of MOD09GA over snow and its ability to discriminate aerosols from those in snow during deposition events have not been assessed. Implicit in MODDRFS is that MOD09GA robustly corrects for aerosols but this should be evaluated in further work to determine this impact.

[27] The nominal footprint of MODIS at nadir is ~463 m but as sensor zenith angle increases so does the area of observation. By the edge of the MODIS scan, the GIFOV reaches 10 times that of nadir [*Dozier et al.*, 2008]. The point spread function further results in overlap at nadir between adjacent observations such that 25% of the signal is from adjacent areas, while only 75% comes from the nominal area [*Tan et al.*, 2006].

[28] Even at the nominal ~463 m footprint, spatial heterogeneity of mountain snow cover makes it rare to find complete snow cover without exposure of some rock, soil, and/or vegetation. Furthermore, geolocation uncertainty of the MODIS grid (~half a pixel for the tiled products - [*Wolfe et al.*, 2002]) can lead to ambiguous comparisons between varying mixtures in MODIS pixels and the corresponding point measurement. In future implementations, we will use the MODDRFS retrievals to feed back on the MODSCAG fractional retrievals for LAI-affected end-members to reduce this uncertainty. Finally, surface roughness of the snow surface (e.g. sastrugi) can modify the HDRF of the snow surface to appear darker in the visible wavelengths than a level or even known surface gradient to the degree that a DEM characterizes this gradient. As such, application of MODDRFS to polar regions where sastrugi occupy vast areas, SZA are large, and LAI concentrations are low should be treated cautiously or not at all.

6. Summary and Discussion

[29] Scientists, policy makers, and resource managers are increasingly aware of the potential impacts of radiative forcing by LAI in snow and ice relative to glacier mass balance, regional hydrology, and climate. MODDRFS reduces a critical void in our knowledge of the spatial and temporal variations of radiative forcing by LAI around the globe. MODIS' spectral and spatial samplings, coupled with its greater radiometric dynamic range, facilitate this semi-quantitative retrieval not available from its predecessor (AVHRR, Landsat Thematic Mappers) or contemporary (ASTER) spaceborne imagers. MODDRFS is the first regularly produced retrieval of radiative forcing by LAI in snow and is currently being distributed for the western United States and Hindu Kush through Himalaya via the JPL Snow Data Server (http://snow.jpl.nasa.gov/). We are now working on the details of leveraging the instantaneous MODIS retrieval with geostationary retrievals of diurnal at-surface irradiances to generate daily mean radiative forcings by LAI.

[30] Looking forward, more robust quantitative retrieval will come from spaceborne imaging spectrometers such as the NASA Decadal Survey Hyperspectral Infrared Imager (HyspIRI). Its spectral sampling will allow continuous measurement across the spectrum and its 60 m spatial sampling will allow unambiguous retrievals in homogeneous snow.

[31] **Acknowledgments.** This work was funded by NSF grant ATM04323237 and NASA projects NNX10A097G and NNX09A038HS01. Part of this work was performed at the Jet Propulsion Laboratory, California Institute of Technology under a contract with NASA.

[32] The Editor thanks Stephen Warren and an anonymous reviewer for their assistance in evaluating this paper.

References

Barnett, T. P., J. C. Adam, and D. P. Lettenmaier (2005), Potential impacts of a warming climate on water availability in snow-dominated regions, *Nature*, *438*, 303–309, doi:10.1038/nature04141.

Brandt, R. E., S. G. Warren, and A. D. Clarke (2011), A controlled snowmaking experiment testing the relation between black carbon content and reduction of snow albedo, *J. Geophys. Res.*, *116*, D08109, doi:10.1029/2010JD015330.

Conway, H., A. Gades, and C. F. Raymond (1996), Albedo of dirty snow during conditions of melt, *Water Resour. Res.*, *32*, 1713–1718, doi:10.1029/96WR00712.

Dozier, J., T. H. Painter, K. Rittger, and J. E. Frew (2008), Time-space continuity of daily maps of fractional snow cover and albedo from MODIS, *Adv. Water Resour.*, *31*, 1515–1526, doi:10.1016/j.advwatres.2008.08.011.

Flanner, M. G., C. S. Zender, P. G. Hess, N. M. Mahowald, T. H. Painter, V. Ramanathan, and P. J. Rasch (2009), Springtime warming and reduced snow cover from carbonaceous particles, *Atmos. Chem. Phys.*, *9*, 2481–2497, doi:10.5194/acp-9-2481-2009.

Hansen, J., and L. Nazarenko (2004), Soot climate forcing via snow and ice albedos, *Proc. Natl. Acad. Sci. U. S. A.*, *101*, 423–428, doi:10.1073/pnas.2237157100.

Howat, I. M., and S. Tulaczyk (2005), Climate sensitivity of spring snowpack in the Sierra Nevada, *J. Geophys. Res.*, *110*, F04021, doi:10.1029/2005JF000356.

Kaspari, S., P. A. Mayewski, M. Handley, S. Kang, S. Hou, S. Sneed, K. Maasch, and D. Qin (2009), A high-resolution record of atmospheric dust composition and variability since A.D. 1650 from a Mount Everest ice core, *J. Clim.*, *22*, 3910–3925, doi:10.1175/2009JCLI2518.1.

Kaspari, S. D., M. Schwikowski, M. Gysel, M. G. Flanner, S. Kang, S. Hou, and P. A. Mayewski (2011), Recent increase in black carbon concentrations from a Mt. Everest ice core spanning 1860–2000 AD, *Geophys. Res. Lett.*, *38*, L04703, doi:10.1029/2010GL046096.

Mote, P. W., A. F. Hamlet, M. P. Clark, and D. P. Lettenmaier (2005), Declining mountain snowpack in western North America, *Bull. Am. Meteorol. Soc.*, *86*, 39–49, doi:10.1175/BAMS-86-1-39.

Neff, J. C., A. P. Ballantyne, G. L. Farmer, N. M. Mahowald, J. L. Conroy, C. C. Landry, J. T. Overpeck, T. H. Painter, C. R. Lawrence, and R. L. Reynolds (2008), Increasing eolian dust deposition in the western United States linked to human activity, *Nat. Geosci.*, *1*, 189–195, doi:10.1038/ngeo133.

Painter, T. H., A. P. Barrett, C. C. Landry, J. C. Neff, M. P. Cassidy, C. R. Lawrence, K. E. McBride, and G. L. Farmer (2007), Impact of disturbed desert soils on duration of mountain snow cover, *Geophys. Res. Lett.*, *34*, L12502, doi:10.1029/2007GL030284.

Painter, T. H., K. Rittger, C. McKenzie, P. Slaughter, R. E. Davis, and J. Dozier (2009), Retrieval of subpixel snow covered area, grain size, and albedo from MODIS, *Remote Sens. Environ.*, *113*, 868–879, doi:10.1016/j.rse.2009.01.001.

Painter, T. H., J. S. Deems, J. Belnap, A. F. Hamlet, C. C. Landry, and B. Udall (2010), Response of Colorado River runoff to dust radiative forcing in snow, *Proc. Natl. Acad. Sci. U. S. A.*, *107*, 17,125–17,130, doi:10.1073/pnas.0913139107.

Painter, T. H., S. M. Skiles, J. S. Deems, A. C. Bryant, and C. C. Landry (2012), Dust radiative forcing in snow of the Upper Colorado River Basin: 1. A 6 year record of energy balance, radiation, and dust concentrations, *Water Resour. Res.*, *48*, W07521, doi:10.1029/2012WR011985.

Qian, Y., W. I. Gustafson, L. R. Leung, and S. J. Ghan (2009), Effects of soot-induced snow albedo change on snowpack and hydrological cycle in western United States based on Weather Research and Forecasting chemistry and regional climate simulations, *J. Geophys. Res.*, *114*, D03108, doi:10.1029/2008JD011039.

Ramanathan, V., M. V. Ramana, G. Roberts, D. Kim, C. Corrigan, C. Chung, and D. Winker (2007), Warming trends in Asia amplified by brown cloud solar absorption, *Nature*, *448*, 575–578, doi:10.1038/nature06019.

Schaepman-Strub, G., M. Schaepman, T. H. Painter, S. Dangel, and J. V. Martonchik (2006), Reflectance quantities in optical remote sensing—

Definitions and case studies, *Remote Sens. Environ.*, *103*, 27–42, doi:10.1016/j.rse.2006.03.002.

Singh, S. K., A. V. Kulkarni, and B. S. Chaudhary (2010), Hyperspectral analysis of snow reflectance to understand the effects of contamination and grain size, *Ann. Glaciol.*, *51*, 83–88, doi:10.3189/172756410791386535.

Skiles, S. M., T. H. Painter, J. S. Deems, A. C. Bryant, and C. C. Landry (2012), Dust radiative forcing in snow of the Upper Colorado River Basin: 2. Interannual variability in radiative forcing and snowmelt rates, *Water Resour. Res.*, *48*, W07522, doi:10.1029/2012WR011986.

Tan, B., C. E. Woodcock, J. Hu, P. Zhang, M. Ozdogan, D. Huang, W. Yang, Y. Knyazikhin, and R. B. Myneni (2006), The impact of gridding artifacts on the local spatial properties of MODIS data: Implications for validation, compositing, and band-to-band registration across resolutions, *Remote Sens. Environ.*, *105*, 98–114, doi:10.1016/j.rse.2006.06.008.

Thompson, L. G., T. Yao, E. Mosley-Thompson, M. E. Davis, K. A. Henderson, and P.-N. Lin (2000), A high-resolution millennial record of the south Asian monsoon from Himalayan ice cores, *Science*, *289*, 1916–1919, doi:10.1126/science.289.5486.1916.

United Nations Environmental Programme (2011), Integrated assessment of black carbon and tropospheric ozone, 285 pp., Nairobi.

Wake, C. P., and P. A. Mayewski (1994), Modern eolian dust deposition in central Asia, *Tellus, Ser. B*, *46*, 220–233, doi:10.1034/j.1600-0889.1994.t01-2-00005.x.

Warren, S. G., and W. J. Wiscombe (1980), A model for the spectral albedo of snow, II, Snow containing atmospheric aerosols, *J. Atmos. Sci.*, *37*, 2734–2745, doi:10.1175/1520-0469(1980)037<2734:AMFTSA>2.0.CO;2.

Wiscombe, W. J., and S. G. Warren (1980), A model for the spectral albedo of snow, I, Pure snow, *J. Atmos. Sci.*, *37*, 2712–2733, doi:10.1175/1520-0469(1980)037<2712:AMFTSA>2.0.CO;2.

Wolfe, R. E., M. Nishihama, A. J. Fleig, and J. Kuyper (2002), Achieving sub-pixel geolocation accuracy in support of MODIS land science, *Remote Sens. Environ.*, *83*, 31–49, doi:10.1016/S0034-4257(02)00085-8.

CHAPTER 3[2]

IMPACT OF DUST RADIATIVE FORCING IN SNOW ON ACCURACY OF OPERATIONAL RUNOFF PREDICTION IN THE UPPER COLORADO RIVER BASIN

[2] Reprinted with permission of American Geophysical Union. Bryant, A. B., T. H. Painter, J. S. Deems, and S. M. Bender (2013), Impact of dust radiative forcing in snow on accuracy of operational runoff prediction in the Upper Colorado River Basin, *Geophys. Res. Lett.*, *40*, doi: 10.1002/grl.50773, 2013.

GEOPHYSICAL RESEARCH LETTERS, VOL. 40, 1–5, doi:10.1002/grl.50773, 2013

Impact of dust radiative forcing in snow on accuracy of operational runoff prediction in the Upper Colorado River Basin

Ann C. Bryant,[1] Thomas H. Painter,[2] Jeffrey S. Deems,[3,4] and Stacie M. Bender[5]

Received 30 May 2013; revised 18 July 2013; accepted 19 July 2013.

[1] Accurate prediction of snowmelt runoff is critical in the US Intermountain West, where water demand is increasing and snow patterns are shifting. Here, we show that errors in the National Weather Service Colorado Basin River Forecast Center's operational streamflow predictions are correlated with the interannual variability of dust radiative forcing in snow. With data from 2000–2010, we show that errors in snowmelt period streamflow prediction for the southern Colorado Rockies are linearly related to melt period dust radiative forcing in snow as inferred from NASA Moderate Resolution Imaging Spectroradiometer data, which ranged interannually from 20 to 80 W m^{-2}. Each 10 W m^{-2} change of melt period dust forcing resulted in a corresponding change in runoff prediction bias of 10.0% ± 1.5% and a 1.5 ± 0.6 day shift in runoff center of mass. Accounting for bias introduced by dust forcing could improve streamflow prediction in regions prone to dust deposition in the snowpack. **Citation:** Bryant, A. C., T. H. Painter, J. S. Deems, and S. M. Bender (2013), Impact of dust radiative forcing in snow on accuracy of operational runoff prediction in the Upper Colorado River Basin, *Geophys. Res. Lett.*, *40*, doi:10.1002/grl.50773.

1. Introduction

[2] The mountain snowpack of the Upper Colorado River Basin (UCRB) is the primary water source for the Colorado River, which supplies water to seven states and Mexico for agriculture, industry, and domestic consumption [*Barnett and Pierce*, 2009]. Recent studies have shown that dust from the Colorado Plateau shortens snow cover duration at sites in the UCRB by 25–50 days [*Painter et al.*, 2007; *Skiles et al.*, 2012]. Modern dust deposition in the mountains of the UCRB is 5 times greater than prior due to the disturbance of biological and physical crusts in the lowlands of the Western US in the mid nineteenth century [*Neff et al.*, 2008]. By accelerating snowmelt and extending the snow-free season, this impact may have shifted peak normalized runoff at Lee's Ferry, AZ to more than 3 weeks earlier and reduced the total annual runoff of the Colorado River by an average of more than 5% [*Painter et al.*, 2010].

[3] The National Weather Service (NWS) Colorado Basin River Forecast Center (CBRFC) produces operational streamflow forecasts for the Colorado River Basin. The forecasts are produced using the coupled SNOW-17 [*Anderson*, 1976] and Sacramento Soil Moisture Accounting (Sac-SMA) [*Burnash et al.*, 1973] models. Each decade, the coupled models are calibrated to a 30 year historical record of observed streamflow, initiated with mean areal precipitation and mean areal temperature forcings, which are based on observed historical station data. The forcing data are used to build the basin snow water equivalent (SWE) over the snow accumulation period and determine melt volume over the snow ablation period. During the calibration process, model parameters for hundreds of individual forecast points are adjusted so that predicted streamflow most closely matches observations, thus minimizing bias by balancing overestimates and underestimates.

[4] Temperature-index-based models such as SNOW-17 are the central component of operational hydrologic forecasting systems where snowmelt is the dominant influence on regional streamflow [*Franz et al.*, 2008]. Temperature index models assume empirical relationships between air temperature and snowmelt [*Hock*, 2003]. Their low data requirements and simplicity make them the most common tool for snowmelt modeling. However, considerable research dedicated to measuring and modeling snow cover energy and mass balance [*Marks and Dozier*, 1992; *Painter et al.*, 2007] has shown that solar radiation fluxes frequently dominate snowmelt. The temperature index melt factor used by SNOW-17 is a seasonally dependent index of the relative proportions of energy balance components for each elevation zone within a modeled basin [*Anderson*, 2006]. However, the frequency, spatial extent, and mass flux of dust deposition in the UCRB vary annually [*Kavouras et al.*, 2007; *Painter et al.*, 2012; *Steenburgh et al.*, 2012], strongly modifying snow albedo from year to year. As snow surface albedo deviates from the calibration period mean, so does the fraction of incoming shortwave radiation absorbed by the snowpack, directly influencing snowmelt timing and runoff and rendering the melt index less representative.

[5] We know that dust radiative forcing and snowmelt acceleration have considerable interannual variability in the UCRB [*Skiles et al.*, 2012] and hypothesize that this variability affects the accuracy of the CBRFC SNOW-17 predictions. Here, we explore the sensitivity of CBRFC prediction errors to dust radiative forcing as inferred by remote sensing using the NASA Moderate Resolution Imaging Spectroradiometer (MODIS).

Additional supporting information may be found in the online version of this article.

[1]Department of Geography, University of Utah, Salt Lake City, Utah, USA.
[2]Jet Propulsion Laboratory, California Institute of Technology, Pasadena, California USA.
[3]National Snow and Ice Data Center, Boulder, Colorado USA.
[4]NOAA Western Water Assessment, Boulder, Colorado USA.
[5]NOAA/National Weather Service Colorado Basin River Forecast Center, Salt Lake City, Utah, USA.

Corresponding author: A. C. Bryant, Department of Geography, University of Utah, 260 S. Central Campus Dr., Rm. 270, Salt Lake City, UT 84112, USA. (anniebryant@gmail.com)

0094-8276/13/10.1002/grl.50773

Figure 1. The Upper Colorado River Basin with the four gage catchments and their respective 8 digit hydrologic unit code (HUC-8) river basins and stream gages; counterclockwise from the northeast are the Upper Gunnison, Uncompahgre, Upper Dolores, and Animas Basins. DRGC, Animas River at Durango; DRRC, Dolores River below Rico; UCRC, Uncompahgre River near Ridgeway; LFGC, Lake Fork at Gateview.

2. Background

[6] Clean snow has the highest albedo of any naturally occurring Earth surface. When light-absorbing impurities (primarily mineral dust, carbonaceous particles, and organics) are present, snow spectral albedo decreases primarily in the visible wavelengths (VIS), with the effect extending into the near-infrared wavelengths (NIR) as concentration and/or particle single-scattering co-albedo increases [*Painter et al.*, 2007]. We define radiative forcing by dust and/or other light-absorbing impurities in snow in terms of a direct effect and two feedbacks [*Hansen and Nazarenko*, 2004; *Painter et al.*, 2012].

[7] The direct effect comes from the enhanced absorption of solar irradiance by the impurities themselves, primarily in the VIS and to a lesser degree in the NIR [*Warren and Wiscombe*, 1980] and subsequent conductance of that energy directly to the contacting snow grains. The first feedback comes from the enhanced absorption in the NIR and shortwave infrared (SWIR) wavelengths by larger snow grains grown by melt-freeze metamorphism, a process enhanced by the direct effect. This process affects the entire spectrum by reinforcing the direct absorption in the visible wavelengths along with the increased absorption in the NIR through SWIR. The second feedback comes from an extended period of greater absorption of solar radiation by the darker substrate (i.e., soil, rock, and/or vegetation) that is exposed earlier due to the direct effect and first feedback.

[8] Snowpack energy balance and detailed radiation fluxes from micrometeorological stations in southwestern Colorado have provided important insights into the drivers of snowmelt, including how dust changes snowmelt timing [*Painter et al.*, 2007; *Skiles et al.*, 2012; *CSAS*, 2013]. However, there are only three stations throughout the UCRB that provide such measurements and only one other in the western United States with the necessary instrumentation with which to calculate dust radiative forcing. To make up for the paucity of such data, remote sensing data are needed to enable the integration of dust effects with operational hydrologic prediction efforts. Specifically, MODIS data have enabled analysis of snow properties in remote mountain environments [*Painter et al.*, 2009], due to the sensor's dynamic range in the visible wavelengths [*Dozier and Painter*, 2004]. *Painter et al.* [2012] used MODIS data and a coupled radiative transfer model to create the MODIS Dust Radiative Forcing in Snow (MODDRFS) product, which provides per-pixel (463 m) radiative forcing by dust in snow attributed to the "direct effect." Estimates of surface radiative forcing (W m^{-2}) from MODDRFS are determined by multiplying local potential spectral irradiance by the albedo differences between the measured MODIS spectrum and the modeled clean snow spectrum for the same optical grain radius (OGR).

[9] In snowmelt-dominated basins, operational streamflow prediction relies on calibrated relationships between measured air temperature and snowmelt. The strong influence of variable dust loading on absorption of solar radiation and snowmelt rate can cause actual conditions to deviate substantially from these calibrations, potentially reducing prediction skill. This research explores sensitivities of streamflow prediction errors to radiative forcing by dust in snow in the southeastern portion of the UCRB from 2000–2010. Specifically, we (1) quantify prediction errors between observed streamflow and the CBRFC-predicted streamflow data produced for the 1981–2010 calibration of the SNOW-17 and Sac-SMA models and (2) present results that suggest that radiative forcing by dust in snow drives first order uncertainty in the predicted streamflow produced by the coupled SNOW-17 and Sac-SMA system. This analysis indicates that runoff predictions in parts of the UCRB could be markedly improved under current implementation if forecasters had spatially extensive dust radiative forcing in snow data that could inform manual adjustments to runoff forecasts. Ultimately, the remotely sensed retrievals can constrain the physically based hydrologic forecast models that are currently under development by the research community and being considered for potential use at NWS River Forecast Centers.

3. Data and Methods

[10] We performed our analysis in the San Juan Mountains of Colorado (Figure 1), where considerable research and monitoring have been conducted on dust radiative forcing and snowmelt acceleration [*Painter et al.*, 2007; *Skiles et al.*, 2012; *Center for Snow and Avalanche Studies* (*CSAS*), 2013], ecosystem response [*Steltzer et al.*, 2009], and long-term changes in dust deposition

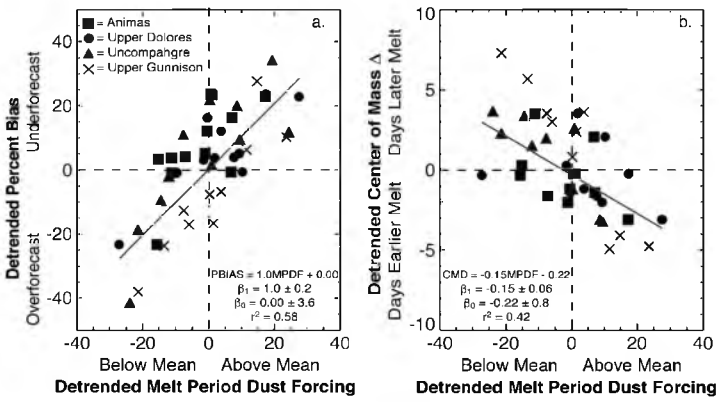

Figure 2. Least squares linear fit of melt period dust forcing and (a) percent bias and (b) center of mass delta with their respective regression coefficient (β_0 and β_1) values.

[*Neff et al.*, 2008]. We used streamflow records from four headwater gages that have no recorded diversions or other obstructions above the gage site. At each gage location, the four rivers have distinct snowmelt-driven peak flows in spring and baseflow for the remainder of the year, often punctuated by small peaks from summer convective precipitation. The catchments for each gage have a maximum elevation near 4000 m and range in area from 272 to 1792 km^2. We refer to each gage catchment by the name of its respective eight digit hydrologic unit code (HUC-8) basin [*Seaber et al.*, 1987]. Lastly, in only one of the basins has forest health been affected by beetle infestation and with markedly minor extent relative to other regions in the UCRB [*United States Forest Service*, 2013], where beetle infestations have altered snow accumulation and melt patterns [*Pugh and Small*, 2012].

3.1. Streamflow Data

[11] We use observed and predicted daily mean streamflow data for each gage between 1 January and 30 September for water years 2000–2010. This span covers the overlapping data record between MODIS and the most recent SNOW-17 and Sac-SMA calibration period. Observed streamflow data were acquired from the US Geological Survey (http://water.usgs.gov) and predicted data were contributed by the CBRFC. Hereafter, we refer to the predicted flows as a product of SNOW-17, acknowledging that predicted snowmelt was input to the Sac-SMA model prior to reaching the basin outlet as predicted streamflow.

3.2. Dust Radiative Forcing in Snow Data

[12] The MODDRFS algorithm [*Painter et al.*, 2012] infers per-pixel radiative forcing by dust in snow using MODIS surface reflectance data and a coupled radiative transfer model for snow. MODDRFS forcings are derived from the spectral differences between the spectral albedo inferred from the measured MODIS spectrum and the modeled clean snow spectral albedo for the same OGR, simulated using the discrete ordinates solution to the radiative transfer equation, all splined to a spectral resolution of 0.01 μm. The spectral difference is multiplied by terrain-corrected local spectral irradiance to obtain surface radiative forcing. The radiative forcing estimate, F, is retrieved from the following:

$$F = \sum_{\lambda=0.35\mu m}^{\lambda=0.876\mu m} E_{\text{corrected},\lambda}\left(\alpha_{\text{clean},\lambda} - \alpha_{\text{MODIS},\lambda}\right)\Delta\lambda, \tag{1}$$

where $E_{\text{corrected}\,\lambda}$ is topographically corrected irradiance at wavelength λ, $\alpha_{\text{clean},\lambda}$ is modeled clean snow spectral albedo of the equivalent OGR, $\alpha_{\text{MODIS},\,\lambda}$ is spectral albedo of the MODIS pixel, and $\Delta\lambda$ is 0.01 μm. The retrieved radiative forcings are instantaneous measurements of dust forcing at the time of MODIS Terra overpass, around 10:30 A.M. local solar time. The root-mean-square error for the MODDRFS retrievals is 32 W m^{-2} with a mean absolute error of 25 W m^{-2} [*Painter et al.*, 2012]. In the Western US, retrieved radiative forcing ranges from 0 to over 400 W m^{-2}.

[13] Each MODDRFS output is masked for cloud cover using a combination of the MODIS cloud mask (embedded in the MOD09GA file) and a user-defined mask, which defines a pixel as cloudy if band reflectances exceed predetermined thresholds. We averaged the MODDRFS outputs to create a daily mean radiative forcing time series for each catchment, $\overline{F_b}$, from

$$\overline{F_b} = \frac{\sum_{\text{pixels}_b} F_i}{n_b}, \tag{2}$$

where F_i is the per-pixel instantaneous forcing, pixels$_b$ are all of the forcing pixels within a given gage catchment, and n_b is the number of forcing pixels within the gage catchment. Lastly, we then averaged the dust forcing for each year and catchment over the rising limb of the hydrograph (starting 1 April, which is the approximate date of peak SWE in the region) to produce the melt period dust forcing (MPDF):

$$\text{MPDF}_b = \frac{\sum_{n=\text{April1}}^{n=\max(Q\text{obs})} \overline{F_b}}{n}, \tag{3}$$

where $max(Q_{\text{obs}})$ is the date of peak observed discharge at each respective stream gage and n is the number of days between 1 April and peak observed streamflow.

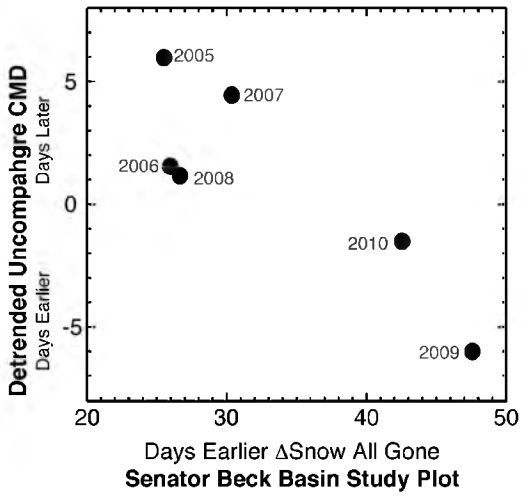

Figure 3. Senator Beck Basin Study Area ΔSAG and center of mass delta for the Uncompahgre gage from 2005 to 2010.

3.3. Statistical Methods

[14] We calculated two metrics to compare the timing and magnitude of predicted relative to observed runoff: percent bias (Pbias) and runoff center of mass (Figure 2). Pbias is a measure of accuracy of a predicted time series [*Franz et al.*, 2008]:

$$\text{Pbias} = \left| \sum_{t=1}^{n} (Q_{\text{obs}}(t) - Q_{\text{sim}}(t)) / \sum_{t=1}^{n} Q_{\text{obs}}(t) \right| \cdot 100. \quad (4)$$

[15] Pbias describes the average tendency of predicted data to be larger or smaller than their observed counterparts, where positive values indicate that the predicted data have an underestimation bias and negative values indicate an overestimation bias. We calculated Pbias over the same interval as MPDF (1 April through peak observed discharge). The runoff center of mass (CM) is the date when half of the total discharge passes the stream gage, accumulated from 1 January to 30 September. The difference between the dates of observed and predicted CM created the variable center of mass delta (CMD), where negative values indicate observed CM occurred earlier than predicted and positive values indicate observed CM occurred later than predicted.

[16] We used simple linear regression techniques to compare radiative forcing by dust in snow (MPDF) to each of the prediction error variables (Pbias and CMD). Pearson's correlation coefficient (r) describes the strength of the linear relationship between MPDF and prediction error. The coefficient of determination (r^2) indicates the proportion of prediction error variance explained by MPDF. Before statistical analysis was performed, however, we removed outliers (z scores greater than 3.0) and any linear trend in MPDF, Pbias, and CMD using the least squares mean line for each variable. The results describe interannual variability over any monotonic change in dust forcing or prediction errors over the analysis period. Results without trends removed are shown in Figures S1 and S2 in the supporting information.

4. Results

[17] MPDF and CMD in the four catchments have significant negative correlation ($\alpha = 0.01$). Each 10 W m^{-2} increase in MPDF results in the observed runoff center of mass occurring 1.5 ± 0.6 days earlier than predicted (Figure 2a), with an r^2 of 0.42. Further, the mean MPDF value for all catchments over the analysis period corresponds to a negligible (0.22 ± 0.8 day per W m^{-2}) difference between observed and predicted in center of mass, suggesting that SNOW-17 is empirically calibrated to the mean forcing over the MODIS record. Thus, deviation from the mean MPDF increases the likelihood that the observed runoff center of mass will not match the predicted.

[18] MPDF had a significant positive correlation with Pbias ($\alpha = 0.01$) and explained the majority of Pbias variance (r^2 of 0.58) in the four catchments, where each 10 W m^{-2} increase of MPDF resulted in a corresponding streamflow prediction bias of 10.0% + 1.5% (Figure 2b). Consistent with CMD, the mean MPDF over all catchments resulted in a negligible Pbias difference (0.0% ± 3.6%) between predicted and observed runoff, where values above the mean resulted in runoff underprediction and runoff overprediction below the mean. Pbias errors in the four catchments ranged from −32% to +49% over the analysis period. Thus, when treated empirically, remotely sensed measurements of dust radiative forcing in snow could potentially allow the CBRFC to reduce the magnitude of prediction errors in these basins to ±20%.

[19] CMD results for the Uncompahgre gage are consistent with snowmelt acceleration attributed to dust on snow in the Senator Beck Basin Study Area (SBBSA), a headwater catchment of the Uncompahgre River [*Painter et al.*, 2007; *Skiles et al.*, 2012; *CSAS*, 2013] (Figure 3). *Skiles et al.* [2012] used the SNOBAL energy balance model [*Marks and Dozier*, 1992] to determine the change in Snow All Gone date (ΔSAG) between modeled clean and dust-influenced snowpacks at SBBSA. CMD at the Uncompahgre gage has a significant relationship (at $\alpha = 0.05$) with ΔSAG from SBBSA, with an $r^2 - 0.75$. With only 6 years of data for a single basin, we proceed cautiously with this relationship. However, it indicates that the 11 year mean MPDF translates to an actual earlier melt of ~25–30 days relative to a clean snowpack and MPDF one standard deviation above the mean translates to ~40–50 days earlier melt.

5. Discussion and Conclusions

[20] The complexity of modeling and measuring snowpack properties in the study basins induces a baseline level of uncertainty in predicted runoff. Changes in basin vegetation from the calibration period, errors in the measurement and interpolation of SNOW-17 input parameters, and limitations of temperature-index-based snowmelt models are all potential sources of error in CBRFC-predicted runoff. Uncertainty is further compounded by the interannual variability in dust deposition that modifies ablation period snow surface albedo, which directly affects snowmelt acceleration [*Painter et al.*, 2007; *Skiles et al.*, 2012]. This research found that SNOW-17 runoff prediction errors are significantly correlated with variability in dust radiative forcing.

[21] Under the current temperature-index-based forecasting paradigm used by the CBRFC, however, the MODDRFS product could be used as a qualitative tool to inform

manual adjustments to runoff forecasts. As we move toward physically based snowmelt runoff models for operations [*National Operational Hydrologic Remote Sensing Center*, 2004], these products can begin to constrain the energy balance components, and variability in radiation fluxes in forested and nonforested regions can be simulated explicitly. Further, MODDRFS retrievals indicate equivalent radiative forcings by dust in other snowmelt- and glacier-melt-dominated hydrologic systems around the world [*Painter et al.*, 2012], such as the mountain snowpacks of Central to South Asia that provide water to over a billion people [*Immerzeel et al.*, 2010]. Future work will include a focus on the hydrologic implications of dust in snow in the Greater Himalaya.

[22] **Acknowledgments.** This work was funded by NASA projects NNX10A097G and NNX09A038HS01 and the NASA Applied Sciences program. Part of this work was performed at the Jet Propulsion Laboratory, California Institute of Technology under a contract with NASA.

[23] The editor thanks Anne Nolin for her assistance in evaluating this paper.

References

Anderson, E. A. (1976), A point energy and mass balance model of a snow cover *NOAA Tech. Rep. NWS, Natl. Oceanic and Atmos. Admin., Silver Spring, Md., 19*.

Anderson, E. A. (2006), Snow accumulation and ablation model—SNOW 17, *User's Guide, US Dept. of Commerce Silver Spring, MD*.

Barnett, T. P., and D. W. Pierce (2009), Sustainable water deliveries from the Colorado River in a changing climate, *Proc. Natl. Acad. Sci. U. S. A., 106*, 7334–7338, doi:10.1073/pnas.0812762106.

Burnash, R. J., R. L. Ferral, and R. A. McGuire (1973), A generalized streamflow simulation system conceptual modeling for digital computers, *U.S. Department of Commerce National Weather Service and State of California Department of Water Resources*.

Center for Snow and Avalanche Studies (CSAS) (2013), http://www.snowstudies.org/.

Dozier, J., and T. H. Painter (2004), Multispectral and hyperspectral remote sensing of alpine snow properties, *Annu. Rev. Earth Planet. Sci., 32*, 465–494, doi:10.1146/annurev.earth.32.101802.120404.

Franz, K. J., T. S. Hogue, and S. Sorooshian (2008), Operational snow modeling: Addressing the challenges of an energy balance model for National Weather Service forecasts, *J. Hydrol., 360*, 48–66, doi:10.1016/j.jhydrol.2008.07.013.

Hansen, J., and L. Nazarenko (2004), Soot climate forcing via snow and ice albedos, *Proc. Natl. Acad. Sci. U. S. A., 101*, 423–428, doi:10.1073/pnas.2237157100.

Hock, R. (2003), Temperature index melt modelling in mountain areas, *J. Hydrol., 282*, 104–115.

Immerzeel, W. W., L. P. H. van Beek, and M. F. P. Bierkens (2010), Climate change will affect the Asian water towers, *Science, 328*, 1382–1385, doi:10.1126/science.1183188.

Kavouras, I. G., V. Etyemezian, J. Xu, D. W. DuBois, M. Green, and M. Pitchford (2007), Assessment of the local windblown component of dust in the western United States, *J. Geophys. Res., 112*, D08211, doi:10.1029/2006jd007832.

Marks, D., and J. Dozier (1992), Climate and energy exchange at the snow surface in the alpine region of the Sierra Nevada 2. Snow cover energy balance, *Water Resour. Res., 28*, 3043–3054.

Neff, J. C., A. P. Ballantyne, G. L. Farmer, N. M. Mahowald, J. L. Conroy, C. C. Landry, J. T. Overpeck, T. H. Painter, C. R. Lawrence, and R. L. Reynolds (2008), Increasing eolian dust deposition in the western United States linked to human activity, *Nat. Geosci., 1*, 189–195, doi:10.1038/ngeo133.

National Operational Hydrologic Remote Sensing Center (2004), *Snow Data Assimilation System (SNODAS) Data Products at NSIDC*, edited by N. S. a. I. D. Center, National Snow and Ice Data Center, Boulder, doi:10.7265/N5TB14TC.

Painter, T. H., A. P. Barrett, C. C. Landry, J. C. Neff, M. P. Cassidy, C. R. Lawrence, K. E. McBride, and G. L. Farmer (2007), Impact of disturbed desert soils on duration of mountain snow cover, *Geophys. Res. Lett., 34*, L12502, doi:10.1029/2007GL030284.

Painter, T. H., K. Rittger, C. McKenzie, P. Slaughter, R. E. Davis, and J. Dozier (2009), Retrieval of subpixel snow covered area, grain size, and albedo from MODIS, *Remote Sens. Environ., 113*, 868–879, doi:10.1016/j.rse.2009.01.001.

Painter, T. H., J. S. Deems, J. Belnap, A. F. Hamlet, C. C. Landry, and B. Udall (2010), Response of Colorado River runoff to dust radiative forcing in snow, *Proc. Natl. Acad. Sci. U. S. A., 107*, 17,125–17,130, doi:10.1073/pnas.0913139107.

Painter, T. H., A. C. Bryant, and S. M. Skiles (2012), Radiative forcing by light absorbing impurities in snow from MODIS surface reflectance data, *Geophys. Res. Lett., 39*, L17502, doi:10.1029/2012gl052457.

Pugh, E., and E. Small (2012), The impact of pine beetle infestation on snow accumulation and melt in the headwaters of the Colorado River, *Ecohydrology, 5*, 467–477, doi:10.1002/eco.239.

Seaber, P. R., F. P. Kapinos, and G. L. Knapp (1987), Hydrologic unit maps: US Geological Survey water supply paper 2294, US Geological Survey.

Skiles, S. M., T. H. Painter, J. S. Deems, A. C. Bryant, and C. C. Landry (2012), Dust radiative forcing in snow of the Upper Colorado River Basin: Part II. Interannual variability in radiative forcing and snowmelt rates, *Water Resour. Res., 48*, W07522, doi:10.1029/2012WR011986.

Steenburgh, W. J., J. D. Massey, and T. H. Painter (2012), Episodic dust events of Utah's Wasatch Front and adjoining region, *J. Appl. Meteorol. Climatol., 51*, 1654–1669, doi:10.1175/JAMC-D-12-07.1.

Steltzer, H., C. C. Landry, T. H. Painter, J. Anderson, and E. Ayres (2009), Biological consequences of earlier snowmelt from desert dust deposition in alpine landscapes, *Proc. Natl. Acad. Sci. U. S. A., 106*, 11,629–11,634, doi:10.1073/pnas.0900758106.

United States Forest Service (2013), 2000–2012 Mountain pine beetle and spruce beetle activity in Colorado and S. Wyoming, *U.S. Forest Service 2012 Aerial Forest Health Survey*.

Warren, S. G., and W. J. Wiscombe (1980), A model for the spectral albedo of snow. II. Snow containing atmospheric aerosols, *J. Atmos. Sci. (USA), 37*, 2734–2745.

CHAPTER 4[3]

DUST RADIATIVE FORCING IN SNOW IN THE UPPER COLORADO RIVER BASIN: INTERPRETATION OF SPATIAL AND TEMPORAL VARIABILITY

4.1 Abstract

The majority of the Colorado River's average annual runoff comes from the high-elevation winter snowpack of the Upper Colorado River Basin's (UCRB) Rocky Mountains. Considerable research has demonstrated that dust deposition on snow in the southeastern portion of the UCRB accelerates snowmelt and snowpack depletion relative to clean snow. Additional research has shown that the magnitude of interannual variability of dust deposition on snow in the southeastern portion of the UCRB is correlated to errors in the National Weather Service Colorado Basin River Forecast Center's (CBRFC) SNOW-17 and Sac-SMA modeled runoff predictions. However, the impacts of dust deposition on snow in other high-elevation regions within the UCRB are not well-quantified. We used the MODIS Dust Radiative Forcing in Snow (MODDRFS) product to estimate the spatial and temporal variability of dust radiative forcing over the full extent of the UCRB between years 2000 and 2010. By analyzing dust forcing in 15

[3] Chapter 4 is a manuscript in preparation for submission to *Water Resources Research*.

subbasins of the UCRB, we found that variability of dust forcing (W m^{-2}) depends on proximity and orientation to the prominent dust emission sources in the Colorado Plateau. Our analysis showed that basins closest to the Colorado Plateau, and along the trajectory of major dust transport, had the highest annual dust forcing and interannual variability of dust forcing. Biases in the operational SNOW-17 streamflow model occur in basins with large interannual variability in dust forcing, resulting in a 6% ± 2% under prediction of streamflow between 2000 and 2010.

4.2 Introduction

The Colorado River flows 2300 km from its headwaters in the Rocky Mountains to the Gulf of California, providing water for municipal use to nearly 40 million people and irrigation for 5.5 million acres of land [*U.S. Dept. of Int.*, 2013]. By 2060, population within the Colorado River Basin (CRB) is expected to grow between 20% and 50% relative to the 2010 population, significantly increasing the commercial and domestic demand for water in the basin [*U.S. Dept. of Int.*, 2013]. The high-elevation snowpack in the Rocky Mountains of the Upper Colorado River Basin (UCRB) contributes roughly 70% of the annual runoff to the Colorado River through spring melt of the winter snow accumulation [*Christensen et al.*, 2004]. Once the snowpack has melted, the water in the UCRB enters the most heavily managed water system in the US where reservoirs, dams, and diversions control the water supply.

The near-total allocation of the Colorado River's water resources [*Christensen et al.*, 2004], and reliance on seasonal snow as the primary source for runoff, make accurate prediction of snowmelt runoff timing and volume critical for downstream users. The

agency charged with monitoring and forecasting streamflow in the UCRB is the National Weather Service (NWS) Colorado Basin River Forecast Center (CBRFC). The CBRFC produces operational streamflow forecasts using the coupled SNOW-17 temperature-index based model [*Anderson*, 1976] and Sacramento Soil Moisture Accounting (Sac-SMA) [*Burnash et al., 1973*] model. Temperature index-based models such as SNOW-17 are the central component of operational hydrologic forecasting systems where snowmelt dominates regional streamflow [*Franz et al.*, 2008]. *Bryant et al.* [2013] showed, however, that the interannual variability of dust deposition on the snowpack in the southeastern portion of the UCRB, and consequent variability of ablation-period snow surface albedo, affects the accuracy of CBRFC streamflow prediction.

While a considerable amount of research has documented the presence [*Painter et al.*, 2007; *Neff et al.*, 2008; *Lawrence et al.*, 2010; *Painter et al.*, 2012b] and consequent impacts [*Painter et al.*, 2007; *Steltzer et al.*, 2009; *Skiles et al.*, 2012; *Bryant et al.*, 2013] of dust on snow in the southeastern part of the UCRB, in other parts of the basin a paucity of data exists. In situ data collection and observations between 2003 and 2013 in western Colorado [*Painter et al.*, 2012b] suggest that dust deposition throughout the basin has considerable spatial and interannual variability. Until recently, however [*Painter et al.*, 2012a], the lack of spatially comprehensive dust forcing data has represented a missing critical input for land-surface modeling [*Dozier et al.*, 2008], which has been constrained to uniform albedo modifications over the UCRB to simulate impacts of basin-wide dust deposition [*Painter et al.*, 2010; *Deems et al.*, 2013]. To better inform modeling efforts and improve operational streamflow forecasting in the UCRB, a more

comprehensive representation of the spatial and temporal patterns of radiative forcing by dust in snow is needed.

Remote sensing can provide spatially continuous data to monitor and measure snowpack properties in mountain environments. The Moderate Resolution Imaging Spectroradiometer (MODIS) in particular, has enabled the analysis of snow properties because its radiometric range in the visible wavelengths does not saturate at the large radiances measured from snow. Using the MODIS Dust Radiative Forcing in Snow (MODDRFS) algorithm [*Painter et al.*, 2012a], this research expands on the analysis of *Bryant et al.* [2013] to (a) infer mean melt-period radiative forcing by dust in snow for 15 high-elevation river basins within the UCRB for years 2000 through 2010, b) show spatial and temporal trends of dust forcing at a variety of scales, and c) analyze impacts on operational streamflow prediction in the UCRB.

4.3 Background

4.3.1 Dust emission, transport, and deposition

Mineral dust is a component in a multitude of climate and Earth system dynamics, such as atmospheric direct radiative forcing from dust [*Sokolik and Toon,* 1996*; Tegen et al.,* 1996], nutrient transport of dust [*Mahowald et al.,* 2009*; Okin et al.,* 2006*; Prospero,* 2002], disturbance and other land-use change [*Belnap and Gillette,* 1997*; Reynolds et al.,* 2010], and ecosystem health [*Field et al.,* 2009]. The distribution and transport of dust are part of a dynamic global system, which includes dust deposition on snow and ice, and in turn an acceleration of the hydrologic cycle. Comprehensive models are able to predict both global and regional distribution of mineral dust in the atmosphere based on

simulation of emission, deposition, and transport processes but the accuracy of these are poorly known [*Grini et al.,* 2005*; Mahowald et al.,* 2003*; Zender et al.,* 2003]. The emission process for dust is driven by wind (given available erodible soils) and the subsequent duration of atmospheric transport is controlled by several factors, of which two are key: (1) size distribution of erodible soil particles and (2) vegetation density and structure that can inhibit dust entrainment [*Reynolds et al.*, 2001; *Okin et al.*, 2006; *Belnap et al.*, 2009]. Dust deposition processes are dry deposition (gravitational sedimentation and turbulent mix-out), and wet deposition (in- and below-cloud scavenging) [*Zender et al.,* 2003].

The largest and most persistent sources of atmospheric dust are located in the northern hemisphere 'dust belt,' which extends from North Africa, over the Middle East, Central and South Asia to China [*Prospero et al.*, 2002]. Atmospheric dust produced in these regions deposit in variable concentrations around the globe as it can be transported thousands of kilometers affecting other regions on intercontinental scales [*Yu et al.*, 2012]. With increasing distance from the source region, the texture of dust becomes finer as the larger particles are removed via gravitational settling. Therefore, dust that reaches the UCRB from the dust-belt region is partially discernable from local sources because of its particle size [*Lawrence et al.*, 2010], which is finer than that deposited from regional dust sources.

Particle size and geochemical analysis strongly suggest that the majority of dust that deposits in winter/spring on the snowpack of the UCRB is characteristic of the adjacent arid and semi-arid regions [*Neff et al.*, 2008; *Reynolds et al.*, 2009; *Lawrence et al.*, 2010]. Synoptic and mesoscale weather systems mobilize and transport large quantities

of dust from the Great Basin and Colorado Plateau tens to hundreds of kilometers [*Painter et al.*, 2007; *Lawrence et al.*, 2010; *CSAS*, 2013], with peak emission between March and June [*Painter et al.*, 2012b]. Spurred by springtime southwesterly wind, the annual frequency, mass loading, and deposition extent of dust emission from these regions varies along with the weather systems that generate them [*Kavouras et al.*, 2007; *Steenburgh et al.*, 2012].

The position of the UCRB mountain snowpack relative to the Colorado Plateau makes it geographically situated to receive dust deposition. While dust emission has been observed throughout recent history, alpine lake sediments collected in the San Juan Mountains, CO [*Neff et al.*, 2008] and in the Uintah Mountains, UT [*Reynolds et al.*, 2009] have found significantly larger dust deposition rates since the western expansion of the United States in the 1800s. Increased dust emissions over this period have been closely linked to anthropogenic disturbances of previously stable soil crusts that greatly increase the likelihood of wind erosion [*Munson et al.*, 2011]. *Brahney et al.* [2013] showed an increasing trend of dust deposition between 1994 and 2010 in the intermountain west, which they attributed to anthropogenic factors including population increase in the Colorado Plateau, increased off-road vehicle usage, and a quadrupling of the number of wells drilled for natural gas extraction. Over the same period, drought conditions dominated significant portions of the Colorado Plateau [*Woodhouse et al.*, 2010], which compounds the impacts of arid-land disturbance [*Neff et al.*, 2005]. Further, it is likely that projected increases in the frequency of drought conditions in the southwestern US and intensification of land use will lead to increased dust emission from the arid and semi-arid regions of the southwest [*Field et al.*, 2009; *Munson et al.*, 2011].

4.3.2 Dust on snow

Radiative forcing by dust in snow is enabled by from two major factors: (i) larger particles (greater than 5.0 μm) tend to accumulate near the snow surface as ablation advances [*Conway et al.*, 1996], and (ii) in the Rocky Mountains in the western-United States, dust arrives and concentrates at the surface during late winter and spring when solar irradiance is increasing [*Painter et al.*, 2007; *Painter et al.*, 2012b]. Radiative forcing by dust in snow is comprised of instantaneous surface-enhanced absorption attributed to a direct effect (absorption of solar radiation by the dust), a 1st feedback (increased absorption in the near infrared (NIR) by larger-grained snow due to an increased rate of snow metamorphism attributed to the direct effect), and second feedback (increased absorption by earlier-exposed substrate due to the direct and first feedback) [*Hansen and Nazarenko*, 2004; *Painter et al.*, 2007]. For this research, we use the term "radiative forcing" to mean the instantaneous surface enhanced absorption due to dust through the combination of the direct effect and the 1st feedback. *Painter et al.* [2013] have found, however, that percolation of snowmelt increases snow grain size at depth away from the surface, mitigating or reversing the 1st feedback as defined above.

The majority of research analyzing the impacts of dust deposition on snow in the western US have focused on the San Juan Mountains, CO in the southeastern region of the UCRB [*Painter et al.*, 2007; *Steltzer et al.*, 2009; *Skiles et al.*, 2012; *Bryant et al.*, 2013]. While the San Juan Mountains are a relatively small portion of the UCRB, the research focused there has given us critical insights into the potential basin-wide impacts of dust on snow. *Painter et al.* [2007] and *Skiles et al.* [2012] showed that dust deposition on the snow in southwestern Colorado shortens snowcover duration by 25 –

50 days. *Steltzer et al.* [2009] showed that the resultant earlier snowmelt from dust could have consequences of delayed phenology resulting in synchronized growth and flowering and the opportunity for altered species interactions, landscape-scale gene transfer via pollination, and nutrient cycling.

While two studies ([*Painter et al.*, 2010; *Deems et al.*, 2013]) have focused on potential basin-wide impacts of dust deposition on snow, they both applied uniform albedo reductions to the snowpack in the UCRB to simulate the impacts of dust. *Painter et al.* [2010] showed dust on snow (based on 2005 – 2008 dust loading in the San Juan Mountains, CO) has brought peak runoff of the Colorado River at Lee's Ferry 3 weeks earlier than pre-Anglo settlement and caused a loss of 5% in total annual runoff. *Deems et al.* [2013] expanded this analysis by using the dust conditions present in the years 2009 and 2010, 2 years of much greater dust loading, and showed snowmelt 6 weeks earlier than predisturbance dust loading and a 6% loss in total runoff. Quantification of spatial and temporal variability of dust forcing within the UCRB would provide more-accurate simulations of the impacts of dust deposition on snow and allow a watershed-scale treatment of this important hydrologic driver.

4.4 Data and Methodology

4.4.1 Geographic setting

The UCRB is the northern portion of the Colorado River Basin above Lee's Ferry, AZ and is made up of two main physiographic provinces: the southern Rocky Mountains and the Colorado Plateau. Within the UCRB, the Rocky Mountains reach over 4,200 meters and transition from rocky summits, to alpine tundra, to mixed conifer forests. The

Colorado Plateau is a mostly-arid landscape with limited plant cover, surrounded by the Rocky Mountains to the north and east, basin and range topography to the west, and the Mogollon Rim, AZ to the south. Individual site-scale analysis, back trajectory analysis, and geospatial and optical satellite imagery suggest that the 'Four-Corners' area is one of the major dust source regions impacting the UCRB snowpack [*Painter et al.*, 2007], along with a multitude of smaller emission sites throughout the rest of the plateau.

For the analysis between dust radiative forcing and streamflow prediction errors, we used 15 snowmelt-dominated headwater basins within the UCRB as our areal units of analysis (Figure 4.1) and refer to each basin by the name of its respective stream gage (Table 4.1). The 15 basins span the latitudinal gradient of the UCRB, with the most-northern basin headwaters at 43° N and the most southern at 37° N. The 4 northern-most basins analyzed were all west of 109° W latitude while the remaining 11 basins were to the east. The high-elevation area of each basin sustains a winter snowpack and is located in the Rocky-Mountain portion of the UCRB. We did not use basins along the west-central edge of the UCRB that drain the southern Wasatch Mountains, as their peak streamflow can often be rain generated and this research only examines snowmelt driven systems. Thus, while the southern Wasatch do sustain high-elevation snowpacks in the winter through early spring that receives dust deposition, our analysis does not take into account potential dust forcing in this region.

Basin polygons were acquired from the Environmental Protection Agency (EPA) Watershed Boundary Program (water.epa.gov). The basins range in size from 66 km^2 to 1968 km^2. Twelve of the basins were chosen in collaboration with the CBRFC as part of the Snow Modeling and Data Assimilation (SMADA) Testbed, which reflects an RFC-

led effort to coordinate snow-related research with development efforts within western-US operational domains. All SMADA basins are headwater basins with no recorded upstream dams or diversions. Of the three additional analysis basins (not included in SMADA), two (TMCC2 and BNRU1) are headwater basins with no upstream dams or diversions. The remaining basin (WRMC2) is also a headwater basins but with moderate upstream regulation from the gage site. We acquired observed daily-mean streamflow from the USGS (http://water.usgs.gov) for each gage between 2000 and 2010, however, we used naturalized streamflow from the CBRFC for WRMC2. The CBRFC produces naturalized streamflow by taking the known quantities of water removed from the stream channel by reservoirs and diversions and adding that volume back into observed streamflow.

4.4.2 MODIS Dust Radiative Forcing in Snow (MODDRFS)

The Moderate Resolution Spectroradiometer (MODIS) has enabled the analysis of snow properties in remote-mountain environments, because its dynamic range in the visible wavelengths accommodates the large radiances measured from snow without saturation. Since clean snow has high reflectance in the near-infrared and low reflectance in the short-wave infrared, it is easily differentiated from other surfaces such as rock and vegetation. Further, when snow reflectance in the visible wavelengths is attenuated by dust, MODIS can detect the reduction of signal while still having a high enough ratio between VIS and NIR bands four and six to be reliably considered snow [*Dozier and Painter*, 2004].

This research used the MODIS Dust Radiative Forcing in Snow (MODDRFS) product [*Painter et al.*, 2012a], which provides a daily-gridded retrieval of (at time of satellite overpass, nominally 10:30 local solar time) radiative forcing by dust in snow. MODDRFS uses MODIS Terra surface reflectance data and a coupled radiative transfer model for snow. MODDRFS determines the difference between the spectral albedo of snow inferred from MODIS and the modeled clean snow spectral albedo of the equivalent optical grain radius, where the difference is taken between 0.350-0.876 μm. The clean snow spectrum is modeled using the discrete ordinates solution to the radiative transfer equation and both measured and modeled spectra are splined to a spectral resolution of 0.01 μm. The spectral difference is multiplied by terrain-corrected local spectral irradiance to obtain surface radiative forcing by dust (W m^{-2}). Lastly, MODDRFS outputs are masked for vegetation and cloud masked using a combination of the MODIS-embedded cloud mask and a user-defined mask based on band-specific reflectance thresholds. The bias-corrected root mean squared error for the MODDRFS data in the UCRB is 32 W m^{-2} with a mean absolute error of 25 W m^{-2} based on validation from two radiation monitoring sites in the Senator Beck Basin Study Area, CO [*Painter et al.*, 2012a]. MODDRFS uncertainties can be attributed to MODIS' course spectral sampling over the VIS and NIR wavelengths and the ~463.3 m ground instantaneous field of view at nadir, which reaches nearly 10 times that at the edge of the scan angle [*Dozier et al.*, 2008; *Painter et al.*, 2012a], leading to mixed pixels that mimic the MODIS spectrum of dirty-snow. Uncertainties from these two factors have not been quantified, but will be a critical step to improving the MODDRFS algorithm in the future. Therefore, this retrieval is semiquantitative, whereas an imaging spectrometer with

contiguous bands across the spectrum and a much higher spatial resolution would allow a more quantitative retrieval [*Painter et al.*, 2013].

4.4.2.1 Melt Period Dust Forcing (MPDF)

We followed methods from *Bryant et al.* [2013] creating a Mean Melt Period Dust Forcing (MPDF) variable, which represents dust forcing over the rising limb of the hydrograph for each year and basin. First, we created a daily-time series of radiative forcing for each year and basin. The number of pixels used to create daily mean dust forcing varied substantially by basin, but the percent of total basin pixels used had significantly less variability (Figure 4.2). Therefore, the percent of each basin that sustains a high-elevation snowpack is relatively consistent across analysis basins. We then averaged the basin dust forcing time series over the rising limb of the hydrograph, which we define as between 1 April (the approximate date of peak SWE in the region) and the date of observed peak streamflow for each basin:

$$MPDF_b = \frac{\sum_{n=April1}^{n=\max(Qobs)} \overline{F}_b}{n} \tag{4.1}$$

where $max(Q_{obs})$ is the date of peak observed discharge at each respective stream gage and n is the number of days between 1 April and peak observed streamflow, and F_b is daily mean radiative forcing per basin. Observed streamflow data were acquired from the US Geological Survey (http://water.usgs.gov). Because MPDF provides a single annual measure of dust forcing per basin over the [*Bryant et al.*, 2013], it is limited to use for broad conclusions about spatial and temporal patterns of dust forcing in the UCRB rising limb of the hydrograph.

4.4.2.2 Maximum Annual Dust Forcing (MADF)

The Maximum Annual Dust Forcing (MADF) variable provides a spatially comprehensive retrieval of dust radiative forcing across the UCRB. In contrast, MPDF can only be calculated for basins with headwater stream gages not impacted by upstream damns or diversions, therefore limiting the number of basins for which it can be derived. The MADF variable is calculated using Hydrologic Unit Code 12 (HUC12) basins within the UCRB, which are a smaller analysis unit than the MPDF basins. First, we created a daily-time series of mean radiative forcing for each basin using MODDRFS retrievals [*Bryant et al.*, 2013]. We then calculated the maximum annual dust radiative forcing over the time series for each basin. We did not calculate MADF for basins with less than 7 days of annual snowcover. The HUC12 basin polygons were acquired from the Environmental Protection Agency (EPA) Watershed Boundary Program (water.epa.gov).

4.4.3 Streamflow prediction errors

The SNOW-17 model used by the CBRFC is a temperature index model that relies on an empirical relationship between air temperature and snowmelt. The model is calibrated to a 30-year historical record of observed streamflow, where model parameters for hundreds of individual forecast points are adjusted so that predicted streamflow most closely matches observations. However, error is introduced into SNOW-17 when actual energy-balance conditions deviate from the calibration-period mean. We use the Percent bias (Pbias) and Absolute Error (AE) metrics to describe the difference between the SNOW-17 predicted streamflow volume (Q_{sim}) and the observed streamflow volume (Q_{obs}). Pbias was calculated as:

$$Pbias = \left[\sum_{t=1}^{n} (Q_{obs}(t) - Q_{sim}(t)) \Big/ \sum_{t=1}^{n} Q_{obs}(t) \right] \bullet 100 \quad (4.2)$$

where positive values indicate a streamflow underprediction and negative values indicate an overprediction [*Franz et al.*, 2008]. We calculated AE as the time integral of the difference between Q_{obs} and Q_{sim} in m^3. Both Pbias and AE were calculated over the same interval as MPDF, for the years 2000 through 2010. Following methods from *Bryant et al.* [2013], we use simple linear regression to compare MPDF with Pbias and AE for each basin. Four of the 15 analysis basins were omitted from these comparisons because of incomplete data records (ENMC2 and BNRU1) and unavailability of predicted streamflow data from CBRFC (TMCC2 and WRMC2). However, the 4 omitted basins were used in the analysis of spatial patterns of MPDF throughout the UCRB.

4.5 Results

The 2000–2010 spatial distributions of MADF (Figure 4.3) and MPDF (Figure 4.4) represent the first measures of radiative forcing by dust in snow throughout the UCRB. While we will discuss the spatial patterns of MADF and MPDF, we will not speak to the detailed atmospheric conditions that control dust transport and deposition in the URCB. Annual MPDF data from 2 analysis basins with incomplete data records (ENMC2 and BNRU1) were included in Figure 4.4, however, their MPDF time series were omitted from statistical analysis of temporal patterns.

4.5.1 MADF variability

The 2000–2010 MADF (Figure 4.3) retrievals represent the first spatially comprehensive measure of maximum annual radiative forcing by dust in snow in the

UCRB. The spatial patterns of MADF appear to be largely influenced by both proximity and orientation to the Colorado Plateau, where the highest annual values are clustered along the western edge of the Colorado Rocky Mountains. The years 2002, 2003, 2006, 2009, and 2010 exhibit the highest MADF values as well as the years with the greatest disparity in MADF between the eastern and western halves of the UCRB. The comprehensive spatial coverage of MADF will provide a critical input to land-surface models that have been constrained to uniform snow albedo modifications over the UCRB to simulate basin-wide dust deposition [*Painter et al.*, 2010; *Deems et al.*, 2013]. Future work will involve determining the existence of temporal trends for each of the basins with MADF values over the 2000-2010 analysis period.

4.5.2 MPDF variability

The 2000–2010 mean MPDF values for each basin suggest three distinct dust-forcing regions within the UCRB (Figure 4.5): Central Basin Region (CBR), Eastern Basin Region (EBR), and the Northern Basin Region (NBR). Annually, the CBR had the highest MPDF values, followed by those in the EBR, and the NBR, respectively. In 8 years of the 11-year analysis period, mean MPDF values for each region were significantly different from each other ($p<0.01$). The other 3 years – 2000, 2001, and 2005 – had the lowest basin-wide MPDF values and the mean MPDF values were not significantly different between regions. Basins within the CBR also had higher interannual variability than those in the EBR and NBR, with mean respective 11-year standard deviations for each region of 14.5 W m^{-2} (CBR), 7.0 W m^{-2} (EBR), and 5.7 W m^{-2} (NBR), with associated MPDF ranges of 43.7 W m^{-2}, 21.2 W m^{-2}, and 18.3 W m^{-2},

respectively. Therefore, there is substantial regional variability of both the magnitude and interannual variability of dust radiative forcing.

MPDF in the CBR increased at a rate of 2.0 W $m^{-2}a^{-1}$ ± 0.45 between 2000 and 2010 ($p<0.001$) (Figure 4.6a) while the EBR and NBR had no significant trend (Figure 4.6b). Interestingly, interannual variations in the CBR and EBR were generally synchronous despite the differences in trend. The NBR MPDF values, in contrast, generally varied independently of the CBR and EBR, perhaps due to a different synoptic dust pattern (e.g., *Steenburgh et al.*, [2012]). However, we hypothesize that the MODDRFS model is not sufficiently sensitive to discern the subtle interannual variability of dust forcing in the NBR. Therefore, relatively small increases in dust deposition on the snowpack could be present and impact on regional hydrology and ecosystem dynamics, but are undetected due to the limitations of the multispectral imagery. A more robust quantitative retrieval is available from the NASA Airborne Visible/Infrared Imaging Spectrometer (AVIRIS). *Painter et al.* [2013] showed that radiative forcing retrieval-errors using AVIRIS were an order of magnitude less than those with MODIS [*Painter et al.*, 2012a]. Since our analysis covers a relatively short period of record, we cannot suggest that trends in MPDF observed between 2000 and 2010 can be extrapolated in time.

4.5.3 MPDF and streamflow prediction error

MPDF was a significant predictor of Pbias in 5 basins located in the CBR. The slope of the regression line for each basin was somewhat similar, indicating a spatially consistent prediction error due to a change in MPDF. MPDF in each of the basins with a significant relationship varied by more than 12 W m^{-2} a^{-1} (Figure 4.7). Of the 6 basins

where MPDF varied less than 12 W m^{-2} a^{-1}, 5 had positive slope values between MPDF and Pbias, however, these relationships were not significant. This finding supports conclusions of *Bryant et al.* [2013] that significant correlation between MPDF and Pbias is dependent upon interannual variability from analysis period mean dust forcing (Figure 4.8). The regression between MPDF and Pbias indicates that the 11-year mean MPDF for the 5 basins in the CBR with significant relationships would have resulted in a 6% ± 2% under-prediction of streamflow for the 2000 to 2010 analysis period.

The total streamflow volume, measured in millions of cubic meters (mcm), that is impacted by dust forcing varies relative to catchment size. The relationship between MPDF and Absolute Error (AE) in the 5 significant basins indicates that the bulk of UCRB prediction error is due to basins in the CBR (Figure 4.9). AE was most sensitive to MPDF in the DRGC2 basin (Figure 4.9), where a unit change (W m^{-2}) in MPDF resulted in an absolute error of 1.93 mcm, effectively equal to the combined errors (2.0 mcm) of the rest of the basins in the CBR. Similarly, a unit change in MPDF in UCRC2, LFGC2, and ALEC2 resulted in two-fold greater AE than DRRC2. The regression between MPDF and AE predicts that the analysis period mean MPDF for the 5 basins with significant relationships in the CBR would have resulted in 2.2 mcm under prediction of streamflow.

4.6 Discussion

4.6.1 Spatial variability

While MADF and MPDF represent different measures of dust radiative forcing, the spatial variability of these metrics is driven by the same first order processes. The spatial

variability of MADF and MPDF can be attributed to dust deposition decreasing with increasing distance from the source region [*Reynolds et al.*, 2001] and that the majority of dust emissions come from the Four Corners region of the Colorado Plateau along a SW to NE trajectory [*Painter et al.*, 2007; *Hallar et al.*, 2011]. Although the scale of these principles varies for any-given dust event, these basic constructs qualitatively explain the general patterns of MADF and MPDF in the UCRB from 2000 to 2010. Further, the high-elevation peaks along the western edge of the Colorado Rocky Mountains provide major physiographic barriers that enhance gravitational settling as well as orographic precipitation and aerosol scavenging [*Lawrence et al.*, 2010] along the trajectory of southwesterly wind driven dust events. Thus increasing the likelihood of high MADF and MPDF values in this region.

We apply the same first-order principles to the regional variability of dust forcing in the CBR, EBR, and NBR. The CBR is the closest region to the dust producing areas of the Colorado Plateau. The EBR is farther downwind and behind the mountain ranges of the CBR along the dominant dust trajectory from the Colorado Plateau, thereby receiving an attenuated mass of dust that has passed over the CBR. While part of the NBR is adjacent to the Colorado Plateau, it is not along the dominant trajectory synoptic flow driving of major dust events. Therefore, while we expect that future changes in aridity, landcover, and landuse in dust source regions would increase dust deposition to the greatest degree in the CBR, their expansion could produce additional dust source regions with the potential to have more significant impacts on the EBR and NBR, assuming the synoptic conditions that drive dust emission do not change.

MADF and MPDF variability over smaller spatial scales can be attributed to a myriad of factors. The relatively short distance that airborne dust travels between the Colorado Plateau and adjacent basins results in deposition amounts that are sensitive to the exact location of the dust source areas relative to synoptic flow [*Luo et al.*, 2003]. Further, there is a scarcity of data quantifying the impact of complex terrain on dust deposition and redistribution (wind-driven saltation and avalanching) in the UCRB. The USGS Rocky Mountain Snowpack Network (RMSN) and the National Atmospheric Deposition Program (NADP), however, provide calcium ion (Ca^{2+}) concentration data as a proxy for dust deposition. Several studies [*Mast et al.*, 2001; *Clow et al.*, 2002; *Brahney et al.*, 2013] have used data from the RMSN and NADP to show significant latitudinal decrease (from south to north) of Ca^{2+} concentrations, which they have attributed to sampling location distance to major dust source regions. While RMSN and NADP provide long records of spatially extensive point measurements of Ca^{2+}, both datasets have shortcomings. Ca^{2+} from the RMSN provide an integrated sample of wet and dry dust deposition, but data are only collected through April 1st [*Clow et al.*, 2002], predating the majority of dust deposition in the UCRB [*Painter et al.*, 2012b]. Conversely, the NADP data are collected over the full snow accumulation and ablation season, however, samplers are used that remain closed to the atmosphere until triggered by precipitation, thus providing only wet-deposition Ca^{2+} concentrations [*Brahney et al.*, 2013].

4.6.2 Temporal variability

MPDF in the CBR increased at a rate of 2.0 W $m^{-2}a^{-1}$ ± 0.45 over the 2000–2010 analysis period. Using the abovementioned NADP Ca^{2+} data, *Brahney et al.* [2013]

independently corroborated that increase, showing an increasing trend of dust deposition in the intermountain west between 1994 and 2010. In both the MPDF and Ca^{2+} time series, annual minimum and maximum dust values were increasing. Therefore, relatively 'clean' years are becoming less clean and relatively dusty years are becoming dustier. *Brahney et al.* [2013] attributed increase in dust deposition to a combination of increased aridity, disturbance, and annual number of high-wind events (> 27.5 m s^{-1}), which lies atop the longer-term increases in dust deposition in the UCRB in the mid-1800s [*Neff et al.*, 2008; *Reynolds et al.*, 2009]. Contemporary trends of increases in average global temperatures and changing precipitation regimes are expected to continue and intensify for decades. These changes will manifest in the southwestern US by expanding deserts to the north and east [*Karl et al.*, 2009], while the potential for wind erosion is projected to increase due to drought-driven loss of vegetation cover [*Munson et al.*, 2011]. Therefore, while dust loading in the UCRB will likely remain spatially variable, it also appears likely to continue its upward trend over coming decades.

4.6.3 Streamflow prediction error

Error in CBRFC operational streamflow prediction is strongly correlated with MPDF [*Bryant et al.*, 2013], indicating that shifts in snowpack energy balance attributed to dust deposition force the relationship between melt and air temperature to deviate from the calibrated average relationship, rendering the melt factor calibration less accurate. The NWS Office of Hydrology [1998] demonstrated similar melt volume prediction errors from SNOW-17 when higher temperatures, higher humidity, and strong winds force large sensible and latent heating, thus increasing melt rate. *Anderson* [2006] showed that cold,

clear sky periods with an 'aged snow surface' or periods of no wind and above-normal air temperature also result in SNOW-17 under-prediction of streamflow. However, it is unlikely that the above mentioned examples have the capacity to shift snowpack energy balance as far from the calibrated mean as dust deposition, where melting-snow visible albedo can decrease from a clean 0.7 to a dusty 0.3 [*Painter et al.*, 2012b], directly modifying absorbed solar irradiance. Therefore, while SNOW-17 model errors are generally normally distributed for each forecast point, the direction and magnitude of those errors can be forced by significant deviations from mean energy balance conditions. Because streamflow prediction errors are not fully explained by changes in MPDF, however, future work is required to better understand and attribute their origin. This may be particularly important for basins within the UCRB where beetle infestations have dramatically altered the forest canopy [*Vanderhoof et al.*, 2013], resulting in a myriad of potential changes to basin hydrology [*Guardiola-Claramonte et al.*, 2011; *Biederman et al.*, 2012].

4.7 Conclusions

We used MODIS Dust Radiative Forcing in Snow data to explore spatial and temporal patterns of dust radiative forcing in the Upper Colorado River Basin. Dust radiative forcing exhibits regional variation driven by proximity and orientation to dust source regions in the Colorado Plateau. Our analysis suggests that the region closest and along the trajectory of major dust transport, had the highest annual dust forcing and interannual variability of dust forcing. Our results reveal that biases in the operational SNOW-17 streamflow model occur in this area where large interannual variability in dust

forcing results in a 6% (2.2 mcm) under-prediction of streamflow between 2000 and 2010. Lastly, we hypothesize that the hydrologic regime in regions with lower interannual variability is still modified by that respective dust, despite not having enough variability to produce a significant component of SNOW-17 errors.

As the CBRFC moves towards more physically-based snowmelt models, MODDRFS could fill a critical data gap in accurately representing snowpack energy balance components. Further, MODDRFS operates in near-real time over the entire UCRB, eliminating the time lag of manual observations and gaps in point measurements. As water demand increases and water supply is projected to decrease, accurate prediction of the timing and volume of snowmelt runoff is critical. Our analysis shows that the information provided by MODDRFS could be used to reduce uncertainties in the SNOW-17 model, thereby reducing the strain on those tasked with monitoring and managing the Colorado River system over a period of growing demand and climatic uncertainty.

4.8 Acknowledgments

This work was funded by NASA projects NNX10A097G and NNX09A038H and the NASA Applied Sciences program.

4.9 References

Anderson, E. A. (1976), A point energy and mass balance model of a snow cover, *NOAA Tech. Rep. NWS, Natl. Oceanic and Atmos. Admin., Silver Spring, Md., 19*.

Anderson, E. A. (2006), Snow accumulation and ablation model—SNOW 17, *User's Guide, US Dept. of Commerce Silver Spring, MD.*

Belnap, J., R. Reynolds, M. Reheis, S. L. Phillips, F. E. Urban, and H. L. Goldstein (2009), Sediment losses and gains across a gradient of livestock grazing and plant

invasion in a cool, semi-arid grassland, Colorado Plateau, USA, *Aeolian Research*, doi: 10.1016/j.aeolia.2009.03.001.

Biederman, J. A., P. D. Brooks, A. A. Harpold, D. J. Gochis, E. Gutmann, D. E. Reed, E. Pendall, and B. E. Ewers (2012), Multiscale observations of snow accumulation and peak snowpack following widespread, insect, induced lodgepole pine mortality, *Ecohydrology*.

Brahney, J., A. P. Ballantyne, C. Sievers, and J. C. Neff (2013), Increasing Ca< sup> 2+</sup> deposition in the western US: The role of mineral aerosols, *Aeolian Research*.

Bryant, A. B., T. H. Painter, J. S. Deems, and S. M. Bender (2013), Impact of dust radiative forcing in snow on accuracy of operational runoff prediction in the Upper Colorado River Basin, *Geophys. Res. Lett.*, *40*, doi: 10.1002/grl.50773, 2013.

Burnash, R. J., R. L. Ferral, and R. A. McGuire (1973), A Generalized Streamflow Simulation System Conceptual Modeling for Digital Computers, *U.S. Department of Commerce National Weather Service and State of California Department of Water Resources,* Report by the Joliet Federal State River Forecasts Center, Sacramento, CA.

Christensen, N. S., A. W. Wood, D. P. Lettenmaier, and R. N. Palmer (2004), Effects of climate change on the hydrology and water resources of the Colorado River Basin, *Journal of Hydroclimatology*, *62*, 337-363.

Clow, D. W., G. P. Ingersoll, M. A. Mast, J. T. Turk, and D. H. Campbell (2002), Comparison of snowpack and winter wet-deposition chemistry in the Rocky Mountains, USA: Implications for winter dry deposition, *Atmospheric Environment*, *36*, 2337-2348.

Conway, H., A. Gades, and C. F. Raymond (1996), Albedo of dirty snow during conditions of melt, *Water Resources Research*, *32*, 1713-1718.

Center for Snow and Avalanche Studies (2013), *Archival Data from Senator Beck Basin Study Area.* http://www.snowstudies.org/.

Deems, J. S., T. H. Painter, J. J. Barsugli, J. Belnap, and B. Udall (2013), Combined impacts of current and future dust deposition and regional warming on Colorado River Basin snow dynamics and hydrology, *Hydrol. Earth Syst. Sc. Disc.*, *10*, 6237-6275.

Dozier, J., and T. H. Painter (2004), Multispectral and hyperspectral remote sensing of alpine snow properties, *Annu. Rev. Earth Pl. Sc.*, *32*, 465-494, doi: 10.1146/annurev.earth.32.101802.120404.

Dozier, J., T. H. Painter, and J. Frew (2008), Smoothing and filtering of daily MODIS maps of fractional snow cover and albedo, *Advances in Water Resources*, *31*, 1515-1526, doi: 10.1016/j.advwatres.2008.08.011.

Field, J. P., J. Belnap, D. D. Breshears, J. C. Neff, G. S. Okin, J. J. Whicker, T. H. Painter, S. Ravi, M. C. Reheis, and R. L. Reynolds (2009), The ecology of dust, *Frontiers in Ecology and the Environment*, doi: 10.1890/090050.

Franz, K. J., T. S. Hogue, and S. Sorooshian (2008), Operational snow modeling: Addressing the challenges of an energy balance model for National Weather Service forecasts, *J. Hydrol.*, *360*, 48-66, doi: 10.1016/j.jhydrol.2008.07.013.

Guardiola-Claramonte, M., P. A. Troch, D. D. Breshears, T. E. Huxman, M. B. Switanek, M. Durcik, and N. S. Cobb (2011), Decreased streamflow in semi-arid basins following drought-induced tree die-off: A counter-intuitive and indirect climate impact on hydrology, *Journal of Hydrology*, *406*, 225-233.

Hallar, A. G., G. Chirokova, I. McCubbin, T. H. Painter, C. Wiedinmyer, and C. Dodson (2011), Atmospheric bioaerosols transported via dust storms in the western United States, *Geophysical Research Letters*, *38*, L17801.

Hansen, J., and L. Nazarenko (2004), Soot climate forcing via snow and ice albedos, *P. Natl. Acad. Sci.*, *101*, 423-428.

Hydrology, O. O. (1998), Northeast Floods of January 1996, NOAA Natural Disaster Survey Report, *Office of Hydrology, National Weather Service, Silver Spring, MD*.

Karl, T. R., J. M. Melillo, and T. C. Peterson (Eds.) (2009), *Global Climate Change Impacts in the United States*, Cambridge University Press, New York, NY, USA.

Kavouras, I. G., V. Etyemezian, J. Xu, D. W. DuBois, M. Green, and M. Pitchford (2007), Assessment of the local windblown component of dust in the western United States, *J. Geophys. Res.*, *112*, D08211, doi: 10.1029/2006jd007832.

Lawrence, C. R., T. H. Painter, C. C. Landry, and J. C. Neff (2010), Contemporary geochemical composition and flux of aeolian dust to the San Juan Mountains, Colorado, United States, *J. Geophys. Res.*, *115*, G03007, doi: 10.1029/2009jg001077.

Luo, C., N. M. Mahowald, and J. Del Corral (2003), Sensitivity study of meteorological parameters on mineral aerosol mobilization, transport, and distribution, *Journal of Geophysical Research: Atmospheres (1984-2012)*, *108*.

Mast, M. A., J. T. Turk, G. P. Ingersoll, D. W. Clow, and C. L. Kester (2001), Use of stable sulfur isotopes to identify sources of sulfate in Rocky Mountain snowpacks, *Atmospheric Environment*, *35*, 3303-3313.

Munson, S. M., J. Belnap, and G. S. Okin (2011), Responses of wind erosion to climate-induced vegetation changes on the Colorado Plateau, *Proceedings of the National Academy of Sciences*, doi: 10.1073/pnas.1014947108.

Neff, J., R. Reynolds, J. Belnap, and P. Lamothe (2005), Multi-decadal impacts of grazing on soil physical and biogeochemical properties in Southeast Utah, *Ecological Applications*, *15*, 87-95.

Neff, J. C., A. P. Ballantyne, G. L. Farmer, N. M. Mahowald, J. L. Conroy, C. C. Landry, J. T. Overpeck, T. H. Painter, C. R. Lawrence, and R. L. Reynolds (2008), Increasing

eolian dust deposition in the western United States linked to human activity, *Nat. Geosci.*, doi: 10.1038/ngeo133.

Okin, G. S., D. A. Gillette, and J. E. Herrick (2006), Multi-scale controls on and consequences of aeolian processes in landscape change in arid and semi-arid environments, *Journal of Arid Environments*, *65*, 253-275, doi: 10.1016/j.jaridenv.2005.06.029.

Painter, T. H., A. P. Barrett, C. C. Landry, J. C. Neff, M. P. Cassidy, C. R. Lawrence, K. E. McBride, and G. L. Farmer (2007), Impact of disturbed desert soils on duration of mountain snow cover, *Geophys. Res. Lett.*, *34*.

Painter, T. H., A. C. Bryant, and S. M. Skiles (2012a), Radiative forcing by light absorbing impurities in snow from MODIS surface reflectance data, *Geophys. Res. Lett.*, *39*, L17502, doi: 10.1029/2012gl052457.

Painter, T. H., J. S. Deems, J. Belnap, A. F. Hamlet, C. C. Landry, and B. Udall (2010), Response of Colorado River runoff to dust radiative forcing in snow, *P. Natl. Acad. Sci.*, *107*, 17125-17130.

Painter, T. H., F. C. Seidel, A. C. Bryant, S. M. Skiles, and K. Rittger (2013), Imaging spectroscopy of albedo and radiative forcing by light absorbing impurities in mountain snow, *Journal of Geophysical Research: Atmospheres*, doi: 10.1002/jgrd.50520.

Painter, T. H., S. Skiles, J. Deems, C. Landry, and A. Bryant (2012b), Dust radiative forcing in snow of the Upper Colorado River Basin: Part I. A 6 year record of energy balance, radiation, and dust concentrations, *Water Resour. Res.*, *48*.

Prospero, J. M., P. Ginoux, O. Torres, S. E. Nicholson, and T. E. Gill (2002), Environmental characterization of global sources of atmospheric soil dust identified with the NIMBUS 7 Total Ozone Mapping Spectrometer (TOMS) absorbing aerosol product, *Rev. Geophys.*, *40*, 1002, doi: 10.1029/2000rg000095.

Reynolds, R., J. Belnap, M. Reheis, P. Lamothe, and F. Luiszer (2001), Aeolian dust in Colorado Plateau soils: Nutrient inputs and recent change in source, *Proceedings of the National Academy of Sciences*, *98*, 7123-7127.

Reynolds, R. L., J. S. Mordecai, J. G. Rosenbaum, M. E. Ketterer, M. K. Walsh, and K. A. Moser (2009), Compositional changes in sediments of subalpine lakes, Uinta Mountains (Utah): Evidence for the effects of human activity on atmospheric dust inputs, *Journal of Paleolimnology*, *44*, 161-175.

Skiles, S. M., T. H. Painter, J. S. Deems, A. C. Bryant, and C. C. Landry (2012), Dust radiative forcing in snow of the Upper Colorado River Basin: Part II. Interannual variability in radiative forcing and snowmelt rates, *Water Resour. Res.*

Steenburgh, W. J., J. D. Massey, and T. H. Painter (2012), Episodic dust events of Utah's Wasatch Front and adjoining region, *J. Appl. Meteorol. Clim.*

Steltzer, H., C. C. Landry, T. H. Painter, J. Anderson, and E. Ayres (2009), Dust-induced early snowmelt synchronizes phenology across an alpine landscape, *P. Natl. Acad. Sci.*, *106*, 11629-11634, doi: 10.1073/pnas.0900758106.

U.S. Dept. of Int., B. o. R. (2013), Colorado River Basin Water Supply and Demand Study, Interim Report No. 1, Technical Report B – Water Supply Assessment, Bureau of Reclamation, US Department of the Interior.

Vanderhoof, M., C. A. Williams, B. Ghimire, and J. Rogan (2013), Impact of mountain pine beetle outbreaks on forest albedo and radiative forcing, as derived from MODIS, Rocky Mountains, USA, *Journal of Geophysical Research: Biogeosciences*, 2013JG002386, doi: 10.1002/jgrg.20120.

Woodhouse, C. A., D. M. Meko, G. M. MacDonald, D. W. Stahle, and E. R. Cook (2010), A 1,200-year perspective of 21st century drought in southwestern North America, *Proceedings of the National Academy of Sciences*, *107*, 21283-21288, doi: 10.1073/pnas.0911197107.

Yu, H., L. A. Remer, M. Chin, H. Bian, Q. Tan, T. Yuan, and Y. Zhang (2012), Aerosols from overseas rival domestic emissions over North America, *Science*, *337*, 566-569.

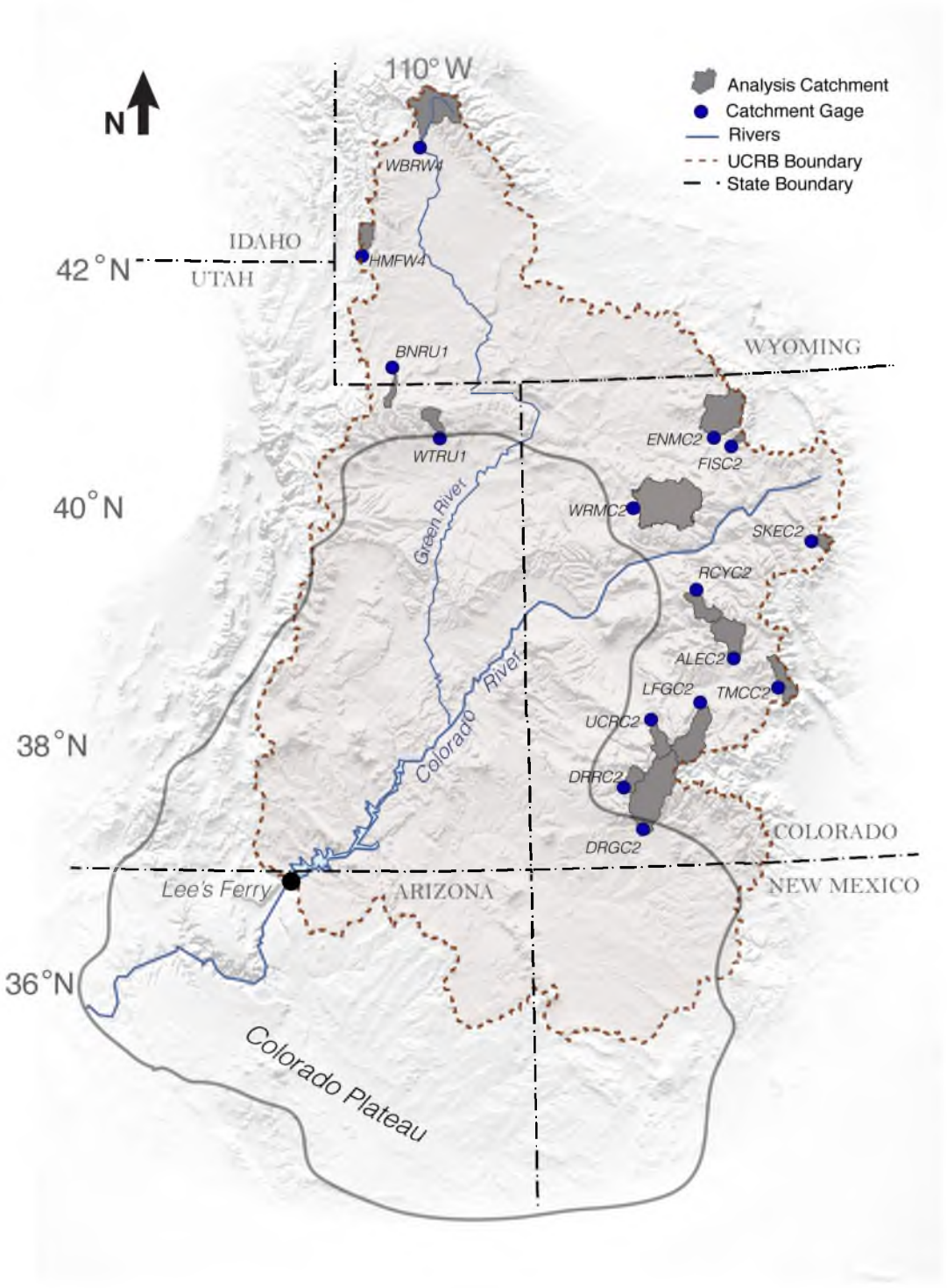

Figure 4.1. Map of Upper Colorado River Basin and individual analysis basins.

Table 4.1. Analysis subbasins arranged by latitude.

Gage Name	Gage ID	HUC	Latitude	Longitude	Drainage Area (SqKm)	MPDF Record
DRGC2	9361500	14080104	37.2792	107.8800	1815.58	2000 - 2010
DRRC2	9165000	14030002	37.6389	108.0600	274.54	2000 - 2010
UCRC2	9146200	14020006	38.1839	107.7450	385.91	2000 - 2010
LFGC2	9124500	14020002	38.2989	107.2290	878.01	2000 - 2010
TMCC2	9115500	14020003	38.3950	106.4230	383.32	2000 - 2010
ALEC2	9112500	14020001	38.6644	106.8480	748.51	2000 - 2010
RCYC2	9081600	14010004	39.2300	107.2270	432.53	2000 - 2010
SKEC2	9047500	14010002	39.6056	105.9420	149.44	2000 - 2010
WRMC2	9304500	14050005	40.0300	107.8620	1968.39	2000 - 2010
FISC2	9238900	14050001	40.4750	106.7860	66.30	2000 - 2010
ENMC2	9242500	14050001	40.5147	106.9540	1160.32	2000 - 2008*
WTRU1	9299500	14060003	40.5936	109.9320	282.31	2000 - 2010
BNRU1	9217900	14040107	40.9592	110.5790	336.70	2002 - 2010*
HMFW4	9223000	14040107	42.1106	110.7100	331.52	2000 - 2010
WBRW4	9188500	14040101	43.0194	110.1370	1212.12	2000 - 2010

*Incomplete gage record.

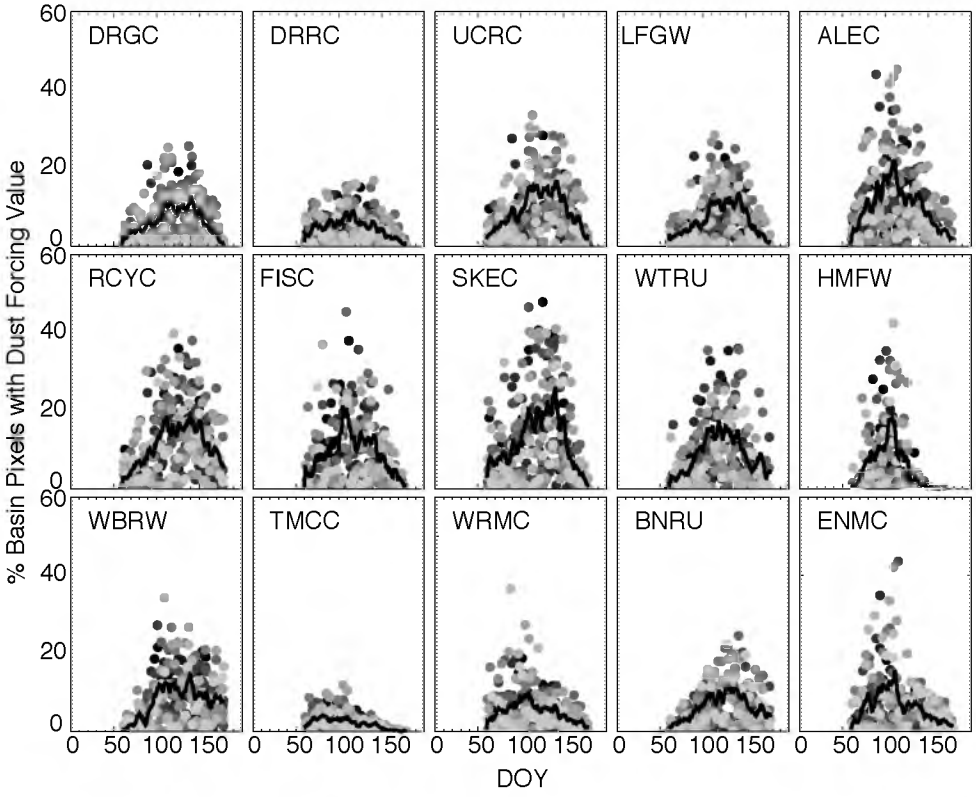

Figure 4.2. Percent of pixels within each analysis basin used to compute daily dust radiative forcing over the analysis period. The thick black line is the mean-daily percent and the circle color distinguishes year.

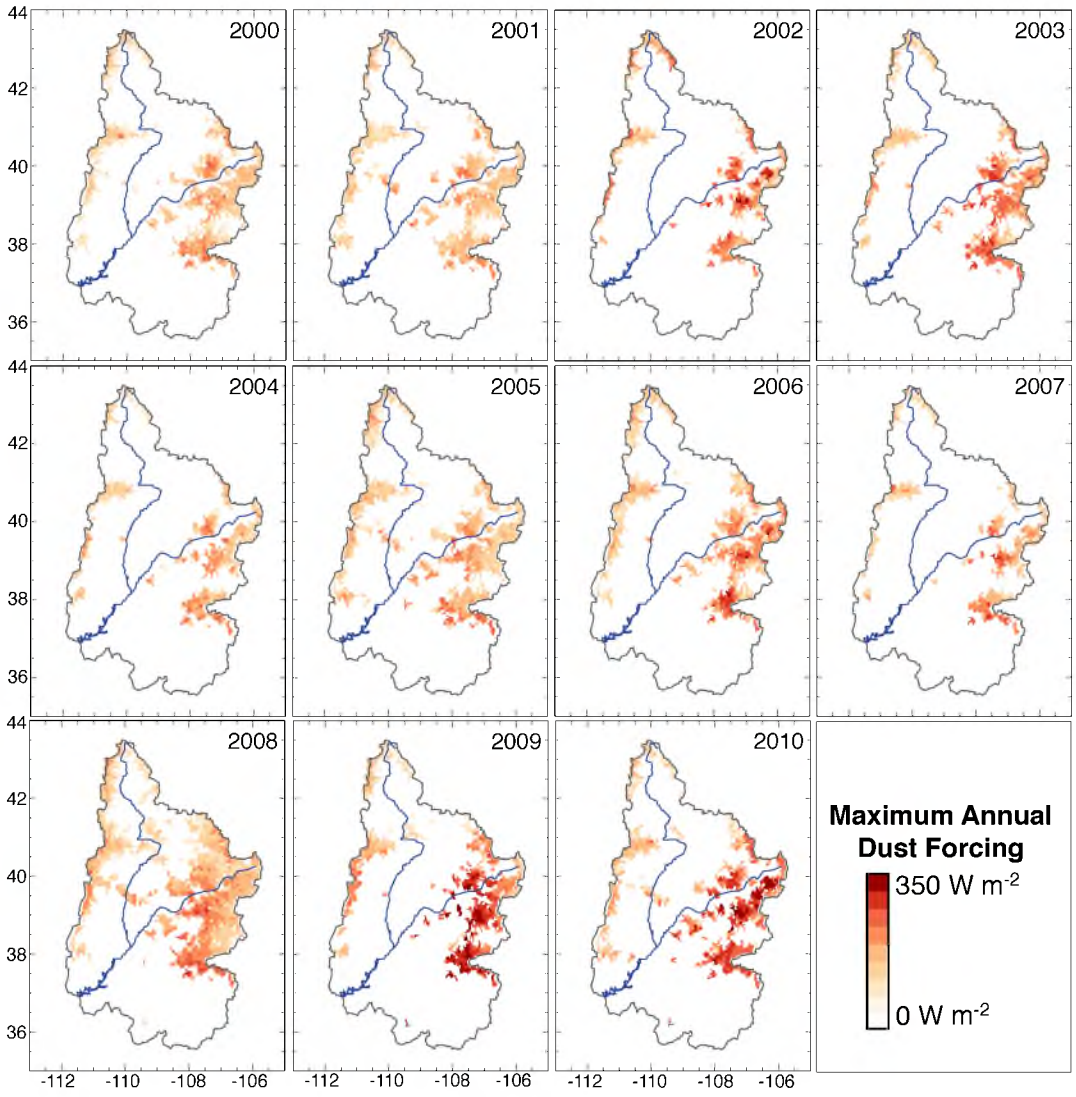

Figure 4.3. Spatial variability of maximum annual dust forcing in the Upper Colorado River Basin where color represents magnitude of maximum annual dust forcing in W m^{-2}.

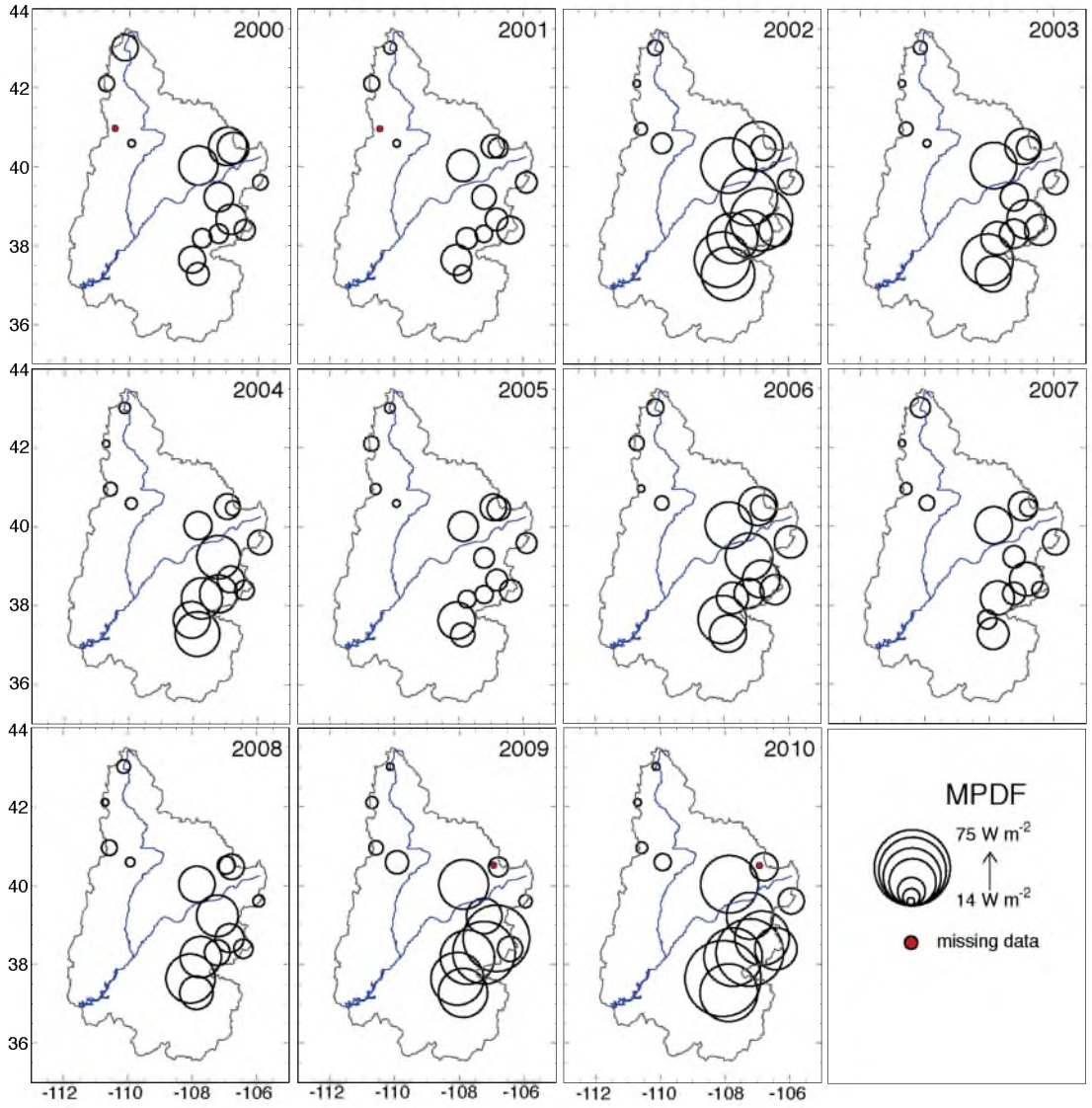

Figure 4.4. Spatial variability of melt period dust forcing in the Upper Colorado River Basin where symbol size represents magnitude of dust forcing in W m^{-2}.

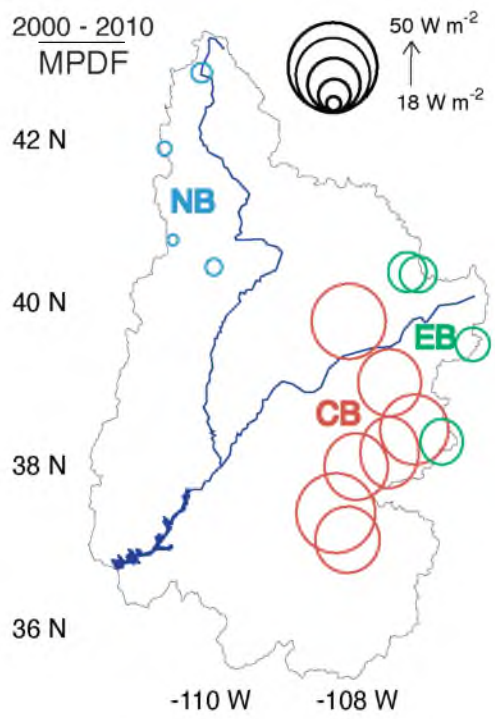

Figure 4.5. 2000–2010 melt period dust forcing, where colors denote the Central Basin region, Eastern Basin region, and Northern Basin region.

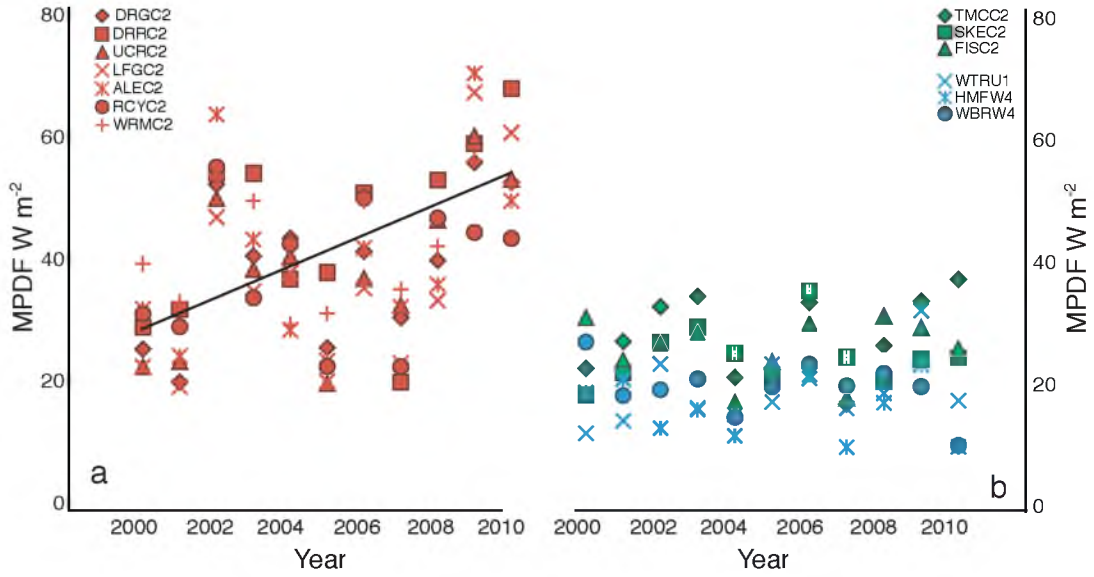

Figure 4.6. 2000–2010 melt period dust forcing for the (left) basins in the Central Basin region and (right) the Eastern and Northern Basin regions.

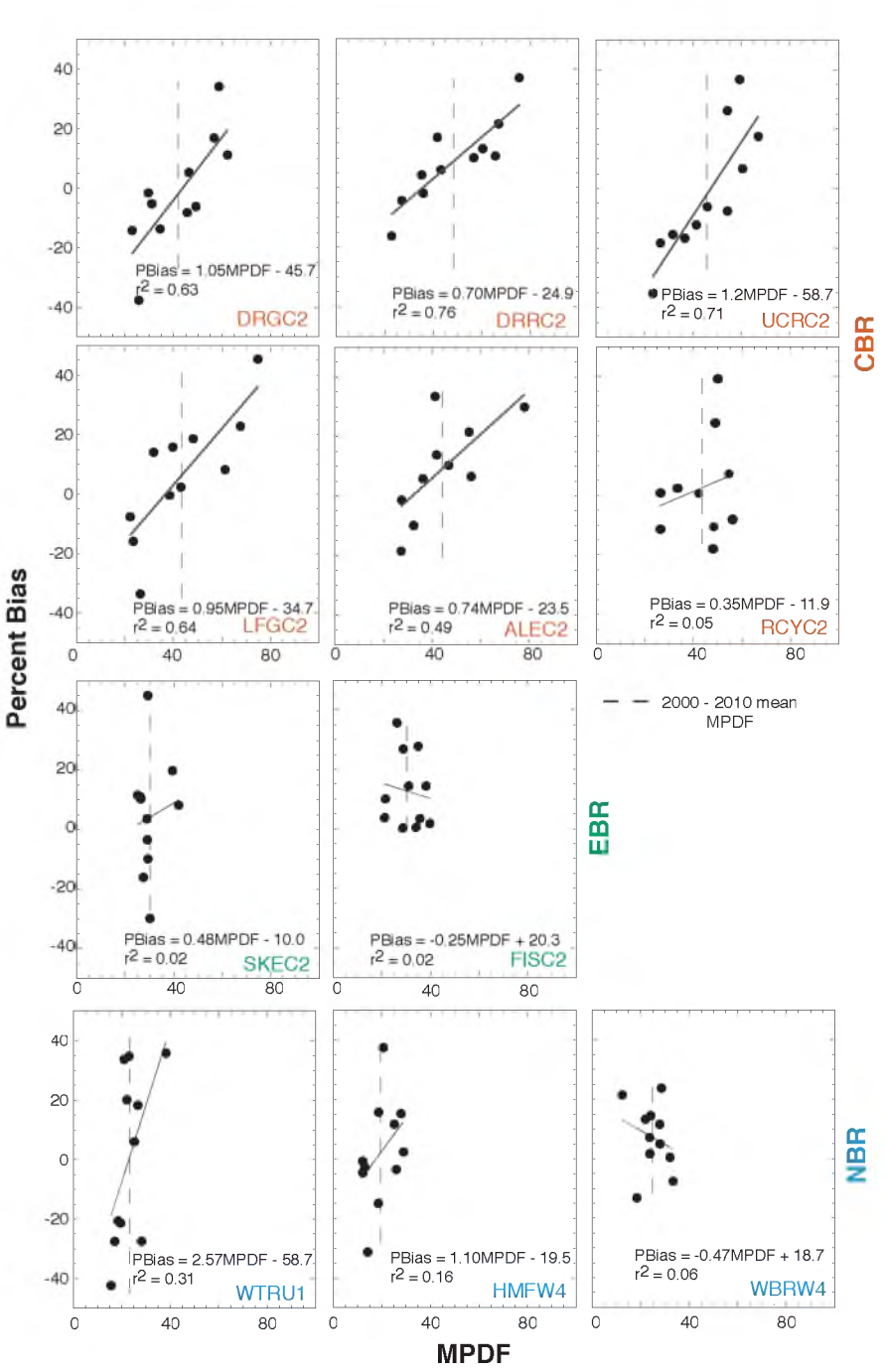

Figure 4.7. Least squares linear fit of melt period dust forcing between 2000–2010 and percent bias streamflow prediction error.

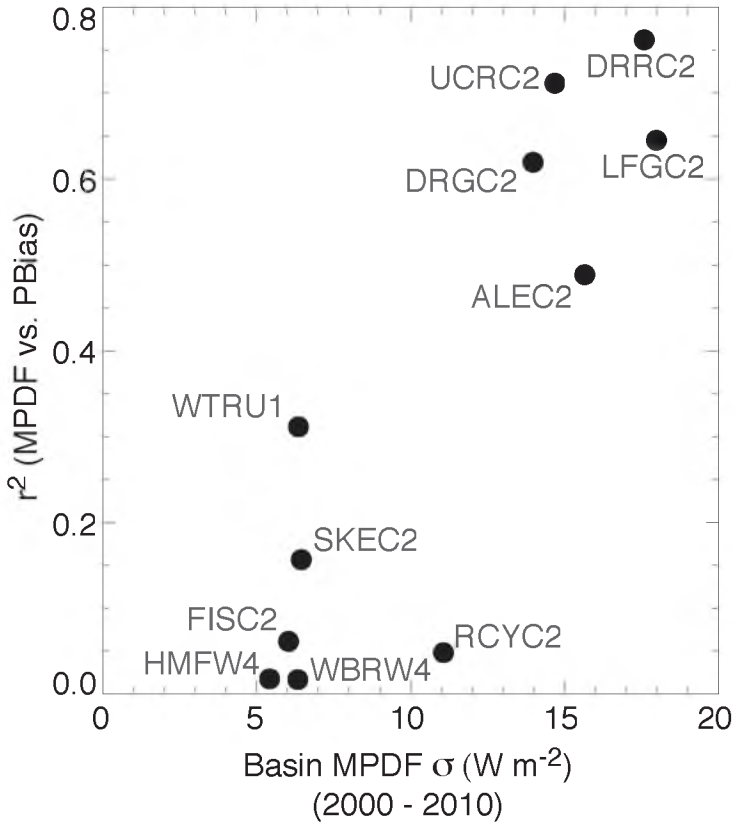

Figure 4.8. Comparison of melt period dust forcing standard deviation and the squared Pearson correlation coefficient between MPDF and percent bias.

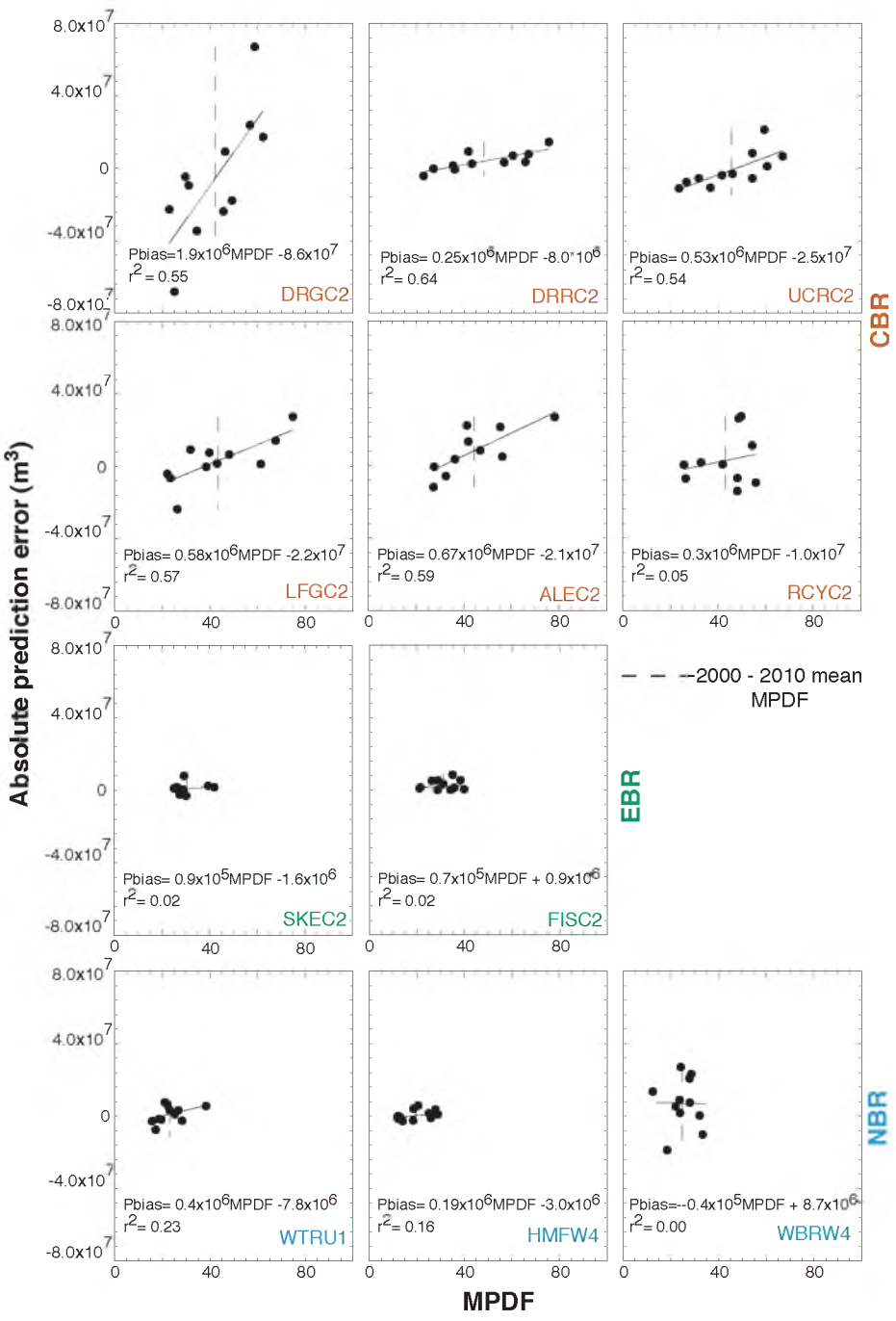

Figure 4.9. Least squares linear fit of melt period dust forcing between 2000–2010 and the absolute error between CBRFC observed and predicted streamflow.

CHAPTER 5

CONCLUSIONS

5.1 Research Contributions

Our MODIS Dust Radiative Forcing in Snow (MODDRFS) product offers a new method to improve streamflow forecasting for an over-allocated river supporting 40 million people. Our analysis has found that radiative forcing of dust in snow is responsible for forecast errors in excess of 60,000 acre feet of water per year and has generated a path towards correcting such errors in the future. The impact of dust radiative forcing on snowmelt has been known, and the monitoring efforts in the Senator Beck Basin Study Area (SBBSA) in the southwestern Colorado have provided substantial insight into the snowpack energy balance in this region. But dust deposition in the UCRB is known to be spatially variable and forcing in the SBBSA is not representative of the UCRB as a whole. Further, SNOW-17 relies on calibrated relationships between temperature and streamflow, which become less reliable in dust-affected basins. Consequently, a real-time spatially distributed model of dust radiative forcing was needed to improve basin-wide streamflow forecasting. This dissertation accomplished this key goal.

The MODDRFS dataset has also revealed patterns of dust radiative forcing that were previously unknown. We have established that the highest annual dust forcing and

highest interannual variability of dust forcing typically occurs along the trajectory of major dust transport in high-elevation areas closest to the Colorado Plateau. We also found that between 2000 and 2010, dust radiative forcing increased in this region at a rate of 2.0 W $m^{-2}a^{-1}$ ± 0.45. Extrapolating this trend in time is not appropriate, but the trend may be due to increasing drought frequency, landuse and landcover changes, in which case, we would expect dust radiative forcing to continue to increase into the future.

5.2 Chapter Conclusions

5.2.1 Chapter 2 results

The MODIS Dust Radiative Forcing in Snow (MODDRFS) retrieval introduced in Chapter 2 reduces a critical void in our knowledge of the spatial and temporal variations of radiative forcing by dust and other light absorbing impurities around the globe. The MODIS Dust Radiative Forcing in Snow (MODDRFS) product is the first remote sensing retrieval to provide daily per-pixel surface radiative forcing (W m^{-2}) by dust in snow-covered regions. The instantaneous MODDRFS retrievals are significantly correlated to dust radiative forcing retrievals from two micrometeorology towers, with an RMSE of 32 W m^{-2} and MAE of 25 W m^{-2}. MODDRFS data are available in near-real time for the western United States, including Alaska, and Hindu Kush through Himalaya via the JPL Snow Data Server (http://snow.jpl.nasa.gov/), where the data archives spans the years 2000-present. These data provide a critical input for scientists, policy makers, and resource managers that are increasingly aware of the impacts of radiative forcing by dust and other light absorbing impurities in snow and ice relative to glacier mass balance [*Painter et al.*, 2013a], regional hydrology [*Bryant et al.*, 2013], and climate [*Hansen and*

Nazarenko, 2004]. In the future, the MODDRFS archive will be appended with a product that will leverage the instantaneous MODDRFS retrieval (at time of MODIS overpass) with geostationary retrievals of diurnal at-surface irradiances to generate daily mean radiative forcings by dust.

5.2.2 Chapter 3 results

The temperature index-based SNOW-17 model is the central component of operational hydrologic forecasting systems when snowmelt dominates streamflow. The temperature index melt factor used by SNOW-17 is a seasonally dependent index of the relative proportions of energy balance components within a modeled basin. However, the frequency, spatial extent, and mass flux of dust deposition in the UCRB vary annually, strongly modifying snow albedo from year to year. As snow surface albedo deviates from the calibration period mean, so does the fraction of incoming shortwave radiation absorbed by the snowpack, directly influencing snowmelt timing and runoff and rendering the melt index less representative. Using a time series of MODDRFS data for 4 basins in the San Juan Mountains of southwestern Colorado, we found that a 10 W m^{-2} increase of dust radiative over the rising limb of the four respective hydrographs, caused the peak observed streamflow to occur 1.5 days earlier than the SNOW-17 predicted peak. Further, we conclude that the MODDFS product could be used as ancillary data to inform manual adjustments to runoff forecasts and, eventually, an input to constrain energy balance components in more physically-based snowmelt runoff models slated to be introduced into operational streamflow prediction in the future.

5.2.3 Chapter 4 results

Using MODIS Dust Radiative Forcing in Snow data, Chapter 4 demonstrated that dust radiative forcing exhibits regional variation driven by proximity and orientation to dust source regions in the Colorado Plateau. Specifically, we showed that the part of the snowpack in the Colorado Rocky Mountains closest to the Colorado Plateau, and along the trajectory of major dust transport, had the highest annual dust forcing and highest interannual variability of dust forcing. Our results also revealed that there was a significant correlation between SNOW-17 driven streamflow predictions and observed streamflow in basins with the highest interannual variability of dust forcing, where large interannual variability in dust forcing resulted in a 6% (2.2 mcm) under prediction of streamflow between 2000 and 2010. We also found that dust radiative forcing over the rising limb of the hydrograph increased at a rate of 2.0 W $m^{-2}a^{-1} \pm 0.45$ between 2000 and 2010. However, because our analysis covers a relatively short period of record, we cannot suggest that trends in MPDF observed between 2000 and 2010 can be extrapolated in time.

5.3 Future Work

5.3.1 MODDRFS beyond the UCRB

The methods developed in this dissertation offer a new opportunity to understand how impurities on snow may be impacting snowmelt in other regions globally. Temperature index models such as SNOW-17 are used widely for a broad range of applications and all may be similarly susceptible to temporal variations in spectral albedo from dust, black carbon, brown carbon, tephra, snow algae, etc.... As such, the progress made here may

help to improve such models and will likely alter our understanding of how impurities are affecting melt globally. Of particular interest, are the MODDRFS radiative forcing retrievals from the high-elevation snowpack of the Hindu Kush through Himalaya (HKH) – an area that provides water to over a billion people [*Immerzeel et al.*, 2010]. We know that dust deposition on mountain snow cover in this region has occurred throughout the present climate record as demonstrated by annual dust layers in high elevation ice cores [*Thompson et al.*, 2000; *Kaspari et al.*, 2009]. However, those cores also reveal that dust concentration increased by as much as a factor of 4 since the 1860s, coinciding with the increased agriculture on the Himalayan plains of Nepal and India [*Thompson et al.*, 2000; *Kaspari et al.*, 2009]. Further, preliminary MODDRFS results from the HKH [*Painter et al.*, 2012], indicate equivalent dust radiative forcing retrievals to those found in the UCRB. Therefore, future work will focus on better understanding the spatial and temporal patterns of dust deposition on snow in the HKH and the consequent impacts on regional hydrology and glaciology.

Lastly, while the majority of this research has focused on the remote sensing of dust deposition on snow, other light absorbing impurities are deposited on snow with enough mass to be detected using satellite imagery. Tephra (airborne pyroclastic accumulation), for example, can deposit on snow as a result of volcanic activity, significantly reducing snow-surface albedo. The eruption of Mt. Redoubt in Alaska in 2009 may have led to exceptionally high glacier mass losses that year due to reduced albedo [*Luthcke et al.*, 2013]. Future work will include assessing the feasibility of using MODDRFS to map tephra extents, such as for the case of Mt. Redoubt.

5.3.2 Beyond MODIS

As new satellite platforms become available we may be able to improve the MODDRFS algorithm enabling higher resolution data that is closer to a true spaceborne quantitative estimate of radiative forcing. Uncertainties may be improved and lower detection thresholds may be attainable. Future work will involve developing MODDRFS-style algorithms for other multispectral instruments that sample in the visible through shortwave infrared spectrum, such as the MODIS replacement instrument Visible Infrared Imaging Radiometer Suite (VIIRS).

The VIIRS instrument is the next generation of multidisciplinary, multispectral sensors to provide global daily surface reflectance measurements to the research and operational communities [*Murphy et al.*, 2001]. Because VIIRS bands in the VIS through SWIR are slightly different than MODIS', and are provided at different pixel resolutions (350 and 750m), we expect the VIIRS dust forcing retrieval to differ from MODDRFS. For example, VIIRS I2 (0.865) and MODIS band 4 (0.856) are centered in the NIR where ice absorption becomes stronger than that of dust. MODDRFS uses MODIS band 4 in the calculation of both NDSI (snow detection) and NDGSI (clean-snow grainsize), assuming it is not impacted by dust. While this assumption generally holds true, heavy dust loading can impact snow spectral reflectance into the NIR, reducing snow spectral reflectance at MODIS band 4. Because VIIRS I2 is centered at slightly longer wavelengths in NIR, were it is less likely to be influenced by dust, it could improve snow detection and grainsize retrieval. Worthwhile future work will involve analyzing the differences between the MODIS and VIIRS dust forcing retrievals, provide important details regarding their sensitivities to pixel size, band location, and bandwidth.

Additionally, spaceborne imaging spectrometers such as the NASA Decadal Survey Hyperspectral Infrared Imager (HyspIRI) will allow continuous measurement across the spectrum, and its 60-meter spatial sampling will reduce the occurrence of mixed pixels, providing an unambiguous retrieval of dust radiative forcing. The quantitative retrieval of dust radiative forcing that comes from Imaging Spectrometer-Snow Albedo and Radiative Forcing (IS-SnARF) algorithm, which uses Airborne Visible/Infrared Imaging Spectrometer (AVIRIS) data [*Painter et al.*, 2013b], can be used to validate future VIIRS and HyspIRI dust radiative forcing retrievals. New satellite products will improve our capacity to retrieve and map dust radiative forcing in remote mountainous regions enabling more informed policy decisions and agreements and enabling future scientific discoveries.

5.4 Closing Remarks

Contemporary trends of increasing temperatures and changing precipitation regimes are expected to continue and intensify for decades. These changes will manifest in the southwestern US by expanding deserts to the north and east of the Colorado Plateau [*Karl et al.*, 2009]. Simultaneously, wind erosion is projected to increase over the same region [*Munson et al.*, 2011]. While dust loading in the UCRB will likely remain temporally and spatially variable, it is also likely to continue its upward trend over time, placing further burden on the Colorado River system and those charged with its management.

This research has shown that datasets such as MODDRFS could significantly improve our ability to monitor and understand snowpack melt dynamics and, therefore, improve CBRFC streamflow forecasts. Currently, CBRFC forecasters manually adjust

daily-simulated streamflow for every forecast point in the UCRB. If they determine that simulated streamflow does not sufficiently match observed streamflow, they modify SNOW-17 inputs and re-run the model. In the coming years, the CBRFC will migrate from SNOW-17 to a more physically based model. At which time, incorporation of a real-time MODDRFS product could significantly reduce forecast errors and the amount of necessary, often subjective, manual streamflow adjustments. Our group should continue working closely with the CBRFC in the coming years, during this transition, to ensure that MODDRFS can be operationalized and updateable as new satellite platforms become available. If done well, this work will constitute a major improvement to forecasting Colorado River flows for years to come.

5.5 References

Bryant, A. B., T. H. Painter, J. S. Deems, and S. M. Bender (2013), Impact of dust radiative forcing in snow on accuracy of operational runoff prediction in the Upper Colorado River Basin, *Geophys. Res. Lett.*, *40*, doi: 10.1002/grl.50773, 2013.

Hansen, J., and L. Nazarenko (2004), Soot climate forcing via snow and ice albedos, *P. Natl. Acad. Sci.*, *101*, 423-428, doi: 10.1073/pnas.2237157100.

Immerzeel, W. W., L. P. H. van Beek, and M. F. P. Bierkens (2010), Climate change will affect the Asian water towers, *Science*, *328*, 1382-1385, doi: 10.1126/science.1183188.

Kaspari, S. D., M. Schwikowski, M. Gysel, M. G. Flanner, S. Kang, S. Hou, and P. A. Mayewski (2009), Recent increase in black carbon concentrations from a Mt. Everest ice core spanning 1860,Äì2000 AD, *Geophysical Research Letters*, *38*.

Luthcke, S. B., T. J. Sabaka, B. D. Loomis, A. A. Arendt, J. J. McCarthy, and J. Camp (2013), Antarctica, Greenland and Gulf of Alaska land-ice evolution from an iterated GRACE global mascon solution, *Journal of Glaciology*, *59*, 613-631.

Murphy, R. E., W. L. Barnes, A. I. Lyapustin, J. Privette, C. Welsch, F. DeLuccia, H. Swenson, C. F. Schueler, P. E. Ardanuy, and P. S. M. Kealy (2001), Using VIIRS to provide data continuity with MODIS, vol. 3, pp. 1212-1214, IEEE, 2001.

Painter, T. H., A. C. Bryant, and S. M. Skiles (2012), Radiative forcing by light absorbing impurities in snow from MODIS surface reflectance data, *Geophys. Res. Lett.*, *39*, L17502, doi: 10.1029/2012gl052457.

Painter, T. H., M. G. Flanner, G. Kaser, B. Marzeion, R. A. VanCuren, and W. Abdalati (2013a), End of the Little Ice Age in the Alps forced by industrial black carbon, *Proceedings of the National Academy of Sciences*, *110*, 15216-15221, doi: 10.1073/pnas.1302570110.

Painter, T. H., F. C. Seidel, A. C. Bryant, S. M. Skiles, and K. Rittger (2013b), Imaging spectroscopy of albedo and radiative forcing by light absorbing impurities in mountain snow, *Journal of Geophysical Research: Atmospheres*, doi: 10.1002/jgrd.50520.

Thompson, L. G., T. Yao, E. Mosley-Thompson, M. E. Davis, K. A. Henderson, and P.-N. Lin (2000), A high-resolution millennial record o the south Asian monsoon from Himalayan ice cores, *Science*, *289*, 1916-1919.